J|A|C|S
ARTICLES
Published on Web 08/07/2002

Investigations by ^{13}C NMR Spectroscopy of Ethene-Initiated Catalytic CO Hydrogenation

Michael L. Turner, Nyoman Marsih, Brian E. Mann, Ruhksana Quyoum, Helen C. Long, and Peter M. Maitlis*

Contribution from the Department of Chemistry, The University of Sheffield, Sheffield S3 7HF, UK

Received March 22, 2002. Revised Manuscript Received June 12, 2002

Abstract: ^{13}C NMR spectroscopy shows that the *n*-alkene and *n*-alkane products from the catalytic hydrogenation of CO in the presence of $^{13}C_2H_4$ probes over Ru/150 °C, Co/180 °C, Fe/220 °C, or Rh/190 °C (1 atm, CO:H_2 1:1, "mild conditions") contain terminal $^{13}CH_3{}^{13}CH_2-$ units. This is consistent with their formation by a regiospecific polymerization of C_1 species derived from CO and initiated by $^{13}C_2H_4$. Although the activities toward individual products differed somewhat, similar distributions and similar product labeling patterns were obtained over all the four catalysts. 1-Butene and the higher 1-*n*-alkenes from all the catalysts were largely $^{13}CH_3{}^{13}CH_2(CH_2)_nCH{=}CH_2$ ($n = 0-3$), propene formed over Ru or Co was $^{13}CH_3{}^{13}CH{=}CH_2$, while both $^{13}CH_3{}^{13}CH{=}CH_2$ and $^{13}CH_2{=}{}^{13}CHCH_3$ were formed over Fe or Rh. Comparison of the conclusions from these probe experiments with those from isotope transient experiments by other workers indicates that the ethene initiator does not significantly modify the course of the CO hydrogenation. The reaction products are largely kinetically determined, and the primary products are mainly linear 1-*n*-alkenes, while the *n*-alkanes and 2-*n*-alkenes largely arise via secondary processes. Since the distribution of products and the labeling in them is so similar, it is concluded that *one basic primary mechanism applies over all the four metals*. Several different reaction paths involving a polymerization of surface methylene, $\{CH_{2(ad)}\}$, have been proposed. Although the predictions based on several of these mechanisms agree with many of the results, the *alkenyl* + $\{CH_{2(ad)}\}$ mechanism, initiated by a surface vinyl $\{CH_2{=}CH_{(ad)}\}$, most easily accommodates the experimental evidence. An alternative path involving sequential addition of surface methylidyne and hydride either to a growing alkylidene chain (*alkylidene* + $\{CH_{(ad)} + H_{(ad)}\}$) or to an alkyl chain (*alkyl* + $\{CH_{(ad)} + H_{(ad)}\}$) has recently been proposed by van Santen and Ciobica. The $\{CH_{2(ad)}\}$ mechanism offers an easier explanation for the formation of the various alkenes, the distribution of products, and of the initiation, while the $\{CH_{(ad)} + H_{(ad)}\}$ mechanism can explain any *n*-alkanes formed as primary products and not derived from alkenes. At higher reaction temperatures over Ru and Co, considerable $^{13}C_1$ incorporation (from natural abundance in the CO and from cleavage of the $^{13}C_2H_4$ probe) was found in all the hydrocarbons. Thus, at higher temperatures $^{13}C_{1(ad)}$ in addition to $^{13}C_{2(ad)}$ species participate in both chain growth and initiation. In summary, adsorbed CO is transformed very easily into surface $C_{1(ad)}$, probably $\{CH_{2(ad)}\}$ in equilibrium with $\{CH_{(ad)}+H_{(ad)}\}$, which act as the propagating species.

Introduction

The hydrogenation of CO over supported metals to 1-alkenes, internal alkenes, and alkanes was discovered by Fischer and Tropsch over 75 years ago[1] and has attracted widespread attention both from the engineering[2] and the chemical[3] points of view. Although Fischer−Tropsch (F−T) today represents "mature technology", interest both in the process and the mechanism has returned in recent years. F−T is now seen as a simple way of utilizing stranded reserves of natural gas and a valuable means for turning natural gas into commodity chemicals (especially α-olefins), as well as into environmentally acceptable liquid hydrocarbon fuels.[4] Large F−T plants are currently operating in South Africa and Malaysia and are being built, or are in advance planning, by major multinationals, in Qatar, Nigeria, Egypt, Indonesia, and Australia; F−T technology becomes competitive at an oil price of ca. US $25/barrel.

The reaction originally described by Fischer and Tropsch was an iron- or cobalt-catalyzed hydrogenation of CO, and over the years a consensus emerged that the F−T reaction is a polymerization of surface CH_2 species derived from CO. Later it was

* Corresponding author. E-mail: P.Maitlis@Sheffield.ac.uk.

(1) Fischer, F.; Tropsch, H. *Brennstoff-Chem.* **1926**, *7*, 97; *Chem. Ber.* **1926**, *59*, 830.

(2) Dry, M. E. *Catalysis Today* **1990**, *6*, 183. Jager, B.; Espinoza, R. *Catalysis Today* **1995**, *23*, 17.

(3) The topic has been extensively reviewed: Anderson, R. B. *The Fischer−Tropsch Reaction*, Academic Press: London, U.K., 1984. Roeper, M. In *Catalysis in C_1 Chemistry*: Keim, W., Ed.; D. Reidel: Dordrecht, The Netherlands, 1983. See also Sheldon, R. A. *Chemicals from Synthesis Gas*, D. Reidel: Dordrecht, The Netherlands, 1983. I. Wender, I.; Sternberg, H. W. *Adv. Catal.* **1957**, *9*, 594. Pichler, H.; Schulz, H. *Chem. Ing. Technol.* **1970**, 42, 1162. Collman, J.; Hegedus, L. S.; Norton, J. R.; Finke, R. G. *Principles and Applications of Organo-Transition Metal Chemistry*; University Science Books: Mill Valley, CA, 1987; p 653.

(4) Romanow, S. *Hydrocarbon Processing* **2001**, *80*, 12. *Los Angeles Times* **2001**, 12 August. *Business Week (Washington, DC)* **1997**, 19 May. *Financial Times (London)* **1997**, 4 February.

10.1021/ja026280v CCC: $22.00

found that ethene (and other olefins) could be added to the syngas with advantage.[5−17] We[18−24] and others[25−29] have shown that C_2 species derived from either vinyl-X (X = Br, SiR_3, etc.) or ethene probes are incorporated into F−T hydrocarbons over a number of metals and indeed that such C_2H_y species are involved in initiating the polymerization.[13−29,30]

A detailed pathway, the basic principles of which stem from concepts originally stated by Fischer and Tropsch, was put forward by Pettit and Biloen and their co-workers.[31,32] The formation of the surface CH_2 was proposed to occur via the coordination and activation of the CO on a metallic site, followed by C−O cleavage and hydrogenation to give, sequentially, surface carbide ($C_{(ad)}$), methylidyne ($CH_{(ad)}$), and methylene ($CH_{2(ad)}$) species[33] (Scheme 1). The last could then be further hydrogenated to surface methyl ($CH_{3(ad)}$) and finally released as methane. Methane formation occurs over all the Fischer−Tropsch-active metals and is the chief process over nickel (Sabatier−Senderens).[34]

Alternatively, the surface methylenes are polymerized to yield linear hydrocarbons, which is the F−T reaction. One popular mechanism for this is the *alkyl* polymerization (*alkyl* + {$CH_{2(ad)}$}) scheme involving the addition of CH_2 to alkyl chains initiated by surface methyl (or hydride, $H_{(ad)}$) terminated by β-elimination of 1-alkene (propene) from the surface alkyl (Scheme 2, after Brady and Pettit[31]).

Scheme 1

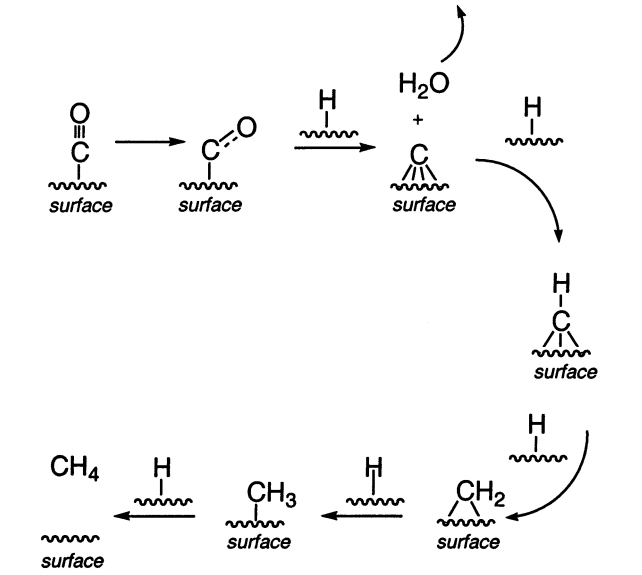

Scheme 2

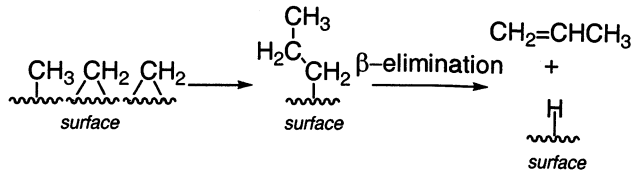

However, this scheme has a number of shortcomings (vide infra) and several alternative proposals have been made. Consideration of the data from our catalytic reactions[18−24] as well as the results of C−C coupling reactions of model organometallic complexes[35,36] led to the *alkenyl* + {$CH_{2(ad)}$} mechanism (Scheme 3), where the chain carriers are surface alkenyl species that react with methylenes.[21,23]

Other proposals with chain propagation by methylene have been suggested to involve surface *alkylidene−hydride* as well as alkenyl intermediates[37] and a metathesis-type mechanism involving *metallacyclobutanes* (vide infra).[38] These three later proposals can also easily accommodate a C_2 initiation, by contrast to the alkyl + {$CH_{2(ad)}$} mechanism. Suggestions have been made concerning the identity of the C_2 initiator: Krishna and Bell[29] proposed it to be a surface ethyl, while Mims and others suggested that it might be a vinylidene (CH_2=C=)[26,28−40] or an ethylidene (CH_3CH=). Our studies, involving both organometallic models and heterogeneous F−T reactions, led to the proposal that the C_2 initiator was a surface *vinyl* (CH_2=CH−), formed from vinyl-X or from ethene (by loss of H) at a

(5) Smith, D. F.; Hawk, C. O.; Golden, P. L. *J. Am. Chem. Soc.* **1930**, *52*, 3221.
(6) Kummer, J. T.; Spencer, W. B.; Podgurski H. H.; Emmett, P. H. *J. Am. Chem. Soc.* **1951**, *73*, 564. Kummer, J. T.; Emmett, P. H. *J. Am. Chem. Soc.* **1953**, *75*, 5177.
(7) Hall, W. K.; Kokes, R. J.; Emmett, P. H. *J. Am. Chem. Soc.* **1960**, *82*, 1027.
(8) Eidus, Ya. T. *Russ. Chem. Rev. (Engl. Transl.)* **1967**, *36*, 338.
(9) Ekerdt, J. G.; Bell, A. T. *J. Catal.* **1980**, *62*, 19.
(10) Schulz; H.; Rao, B R.; Elstner, M. *Erdoel Erdgas, Brennst Chem.* **1970**, *23*, 6512. Schulz, H.; Claeys, M. *Appl. Catal. A General* **1999**, *186*, 71.
(11) Kobori, Y.; Yamasaki, H.; Naito, S.; Onishi, T.; Tamaru, K. *J. Chem. Soc., Faraday Trans. 1* **1982**, *78*, 1473.
(12) Morris, S. R.; Moyes, R. B.; Wells, P. B.; Whyman, R. *J Catal.* **1985**, *96*, 23.
(13) Snel, R.; Espinoza, R. L. *J. Mol. Catal.*, **1987**, *43*, 237.
(14) Boelee, J. H.; Cuesters, J. M. G.; van der Wiele, K. *Appl Catal.* **1989**, *53*, 1.
(15) Adesina, A. A.; Hudgins, R. R.; Silveston, P. L. *Appl Catal.* **1990**, *62*, 295.
(16) Tau, L. M.; Dabbagh, H. A.; Chwala, B.; Davis, B. H. *Catal. Lett*. **1990**, *7*, 141.
(17) Iglesia, E.; Reyes, S C.; Madon, R J.; Soled, S L. *Adv. Catal*. **1993**, *39*, 221.
(18) Ma, F.; Sunley, G. J.; Saez, I. M.; Maitlis, P. M. *J. Chem. Soc., Chem. Commun*. **1990**, 1279.
(19) Turner, M. L.; Byers, P. K.; Long, H. C.; Maitlis, P. M. *J. Am. Chem. Soc*. **1993**, *115*, 4417.
(20) Turner, M. L.; Long, H. C.; Shenton, A.; Byers, P. K.; Maitlis, P. M. *Chem. Eur. J*. **1995**, *1*, 549.
(21) Maitlis, P. M.; Long, H. C.; Quyoum, R.; Turner, M. L.; Wang, Z.-Q. *J. Chem. Soc., Chem. Commun.* **1996**, 1.
(22) Long, H. C.; Turner, M. L.; Fornasiero, P.; Kaspar, J.; Graziani, M.; Maitlis, P. M. *J. Catal*. 1997, **167**, 172.
(23) Maitlis, P. M.; Quyoum, R.; Long, H. C.; Turner, M. L. *Appl. Catal. A: Gen.* **1999**, *186*, 363.
(24) Mann, B. E.; Turner, M. L.; Quyoum, R.; Marsih, N.; Maitlis, P. M. *J. Am. Chem. Soc.* **1999**, *121*, 6497; *J. Am. Chem. Soc.* **2000**, *122*, 1846.
(25) Jordan, D S.; Bell, A T. *J. Phys. Chem.* **1986**, *90*, 4797.
(26) Mims, C. A.; McCandlish, L. E.; Melchior. M. T. *Catal. Lett*. **1988**, *1*, 121; *Proc. Int. Congr. Catal.* **1988**, *4*, 1992; see also Cant, N W.; Bell, A T. *J. Catal*. **1982**, *73*, 257.
(27) Cavalcanti, F. A. P.; Oukaci, R.; Wender, I.; Blackmond, D. G. *J Catal.* **1990**, *123*, 270, and *J Catal*, **1991**, *128*, 311.
(28) Mims, C. A.; Krajewski, J. J.; Rose, K. D.; Melchior, M. T. *Catal. Lett*. **1990**, *7*, 119.
(29) Krishna, K. R.; Bell, A. T. *Proc. 10th Int. Congr. Catal*. **1992**, 181. *Catal. Lett.* **1992**, *14*, 305.
(30) Mims, C. A.; McCandlish, L. E. *J Phys. Chem.* **1987**, *91*, 929.
(31) Brady III, R. C.; Pettit, R. *J. Am. Chem. Soc.* **1980**, *102*, 6181; **1981**, *103*, 1287.
(32) Biloen, P.; *J. R. Neth. Chem. Soc.* 1980, **99**, 33. Biloen, P.; Sachtler, W. M. H. *Adv. Catal.* **1981**, *30*, 165. Biloen, P.; Helle, J. N.; Sachtler, W. M. H. *J. Catal.* **1979**, *58*, 95.
(33) Kaminsky, M. C.; Winograd, N.; Geoffroy, G. L.; Vannice, M. A. *J. Am. Chem. Soc.* **1986**, *108*, 1315. See also, Erley, W.; McBreen, P. H.; Ibach, H. *J Catal*. **1983**, *84*, 229. Klivenyi, G.; Solymosi, F. *Surf. Sci.* **1995**, *342*, 168.
(34) Sabatier, P.; Senderens, J B. *Compt. Rend.* **1902**, *134*, 514 and 689.
(35) Saez, I. M.; Meanwell, N. J.; Taylor, B. F.; Mann, B. E.; Maitlis, P. M. *J. Chem. Soc., Chem. Commun.* **1987**, 361.
(36) Saez, I. M.; Andrews, D. G.; Maitlis, P. M. *Polyhedron* **1988**, *7*, 827. Maitlis, P. M.; Saez, I. M.; Meanwell, N. J.; Isobe, K.; Nutton, A.; Vázquez de Miguel, A.; Bruce, D. W.; Okeya, S.; Bailey, P. M. Andrews, D. G.; Ashton, P. R.; Johnstone, I. R. *New J. Chem.* **1989**, *13*, 419.
(37) Gibson, V C.; Parkin, G.; Bercaw J E. *Organometallics* **1991**, *10*, 220.
(38) Hugues, F.; Besson, B.; Bussiere, P.; Dalmon, J. A.; Basset, J. M.; Olivier, D. *Nouv. J. Chim*. **1981**, *5*, 207.
(39) McCandlish, L. E. *J. Catal*. **1983**, *83*, 362.
(40) Hoel, E. L.; Ansell, G. B.; Leta, S. *Organometallics* **1984**, *3*, 1633; **1986**, *5*, 585.

Scheme 3

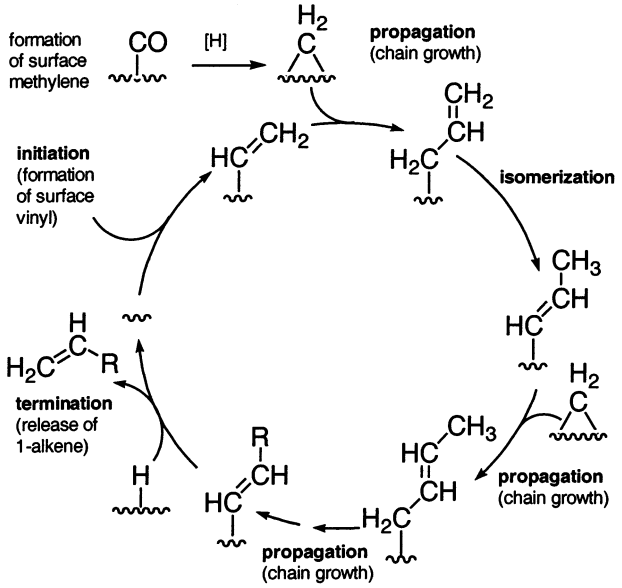

metal center. As we found no evidence for incorporation of C_2 species into the hydrocarbon products using ethyl−Br or $(ethyl)_4Si$ as probes, surface alkyl intermediates seemed less likely.

We here report new studies in which ^{13}C NMR spectroscopy, together with GC−MS and GC,[41] has been used to elucidate the origins and mode of formation of hydrocarbons by hydrogenation of CO in the presence of some ethene.[42] Since the 1-alkene products easily undergo hydrogenation, hydrogen transfer, C−C cleavage, skeletal isomerization, and other equilibration reactions, low pressure (1 atm) and the lowest practicable reaction temperatures for each catalyst were chosen so that secondary reactions were minimized. This has allowed a closer analysis of the *primary* F−T processes.

Our key findings for reactions under relatively *mild conditions*[43] are that (i) the primary products are largely linear 1-alkenes; (ii) different metal catalysts give similar mixtures of hydrocarbon products; (iii) although it influences the amounts of individual products formed, the ethene initiator does not substantially modify the course of the CO hydrogenation; (iv) when the reaction is initiated by a $^{13}C_2H_4$ probe,[44] the *n*-alkene and *n*-alkane products contain terminal $^{13}CH_3{}^{13}CH_2-$ units; and (v) the reactions involve a unidirectional and regiospecific polymerization of C_1H_x species derived from CO and initiated by a surface C_2 species. We also discuss further some of the secondary processes that occur during F−T and that are responsible for a substantial proportion of the linear alkanes and internal olefins produced. At higher reaction temperatures there is considerable and random incorporation into the hydrocarbons of $^{13}C_1$ arising from probe cleavage as well as from natural abundance in the ^{12}CO. The new results allow us to review critically various mechanistic proposals.

Experimental Section

Catalyst Preparation and Pretreatment. A Ru (8%)/SiO_2 catalyst was prepared by incipient wetness impregnation of silica (Davisil grade 645; 60−100 mesh) with a solution of ruthenium trichloride hydrate (PGP Industries (Ireland) Ltd) in methanol, to give a weight loading of 8%.[20] The impregnated sample was dried at 80 °C in air. Prior to CO hydrogenation, the dried sample (1.0 g) was packed into a fixed-bed microreactor (10 cm × 6 mm i.d.), where it was reduced under a steady stream of hydrogen (1 atm, 1000 $cm^3\ h^{-1}$), by programmed heating (4 °C min^{-1}) from room temperature to 400 °C. It was held at 400 °C for 4 h and cooled to the reaction temperature, and then the reaction was started by switching the hydrogen flow to syngas. Similar procedures were used to make 10% Co on silica (from aqueous cobalt nitrate, Fisons AR grade), 10% Fe on silica (from aqueous iron(III) nitrate, Fisons AR grade), and rhodium (8%)/ceria (9%) on silica catalyst [from aqueous rhodium nitrate (Johnson Matthey) and aqueous cerium nitrate (Aldrich)].

Reaction and Analysis. A typical set of reaction conditions used is as follows: the hydrogenation reactions were carried out in a microreactor tube (10 cm × 6 mm i.d.) at 180 °C, 1 atm, H_2:CO = 1, total flow rate 500 $cm^3\ h^{-1}$, unless otherwise stated. After 6−7 h reaction time under syngas, the catalyst required reactivation by reduction under H_2 for 4 h (heating rate 4 °C min^{-1}). A freshly prepared catalyst required two syngas reaction/reactivation cycles followed by 1.5 h on-stream to attain steady-state activity.

Probe Molecule Introduction. Doubly labeled ethene ($^{13}C_2H_4$; Cambridge Isotope Labs., 98% ^{13}C) was used as the probe. The effective ratios of probe to converted CO were as follows: 1:1.6 (Ru/150 °C), 1:4.5 (Ru/165 °C), 1:10 (Ru/180 °C), 1:3.6 (Co/180 °C), 1:7.7 (Co/200 °C), 1:20 (Co/220 °C), 1:3.2 (Rh/190 °C), and 1:6.0 (Fe/220 °C).[45] Several experiments were also carried out using labeled nitromethane ($^{13}CH_3NO_2$, Aldrich) and *n*-propanol ($CH_3CH_2{}^{13}CH_2OH$, Cambridge Isotopes) as probes.

Product Sampling. After catalyst reduction the reactor temperature was reduced to the required value and the hydrogen stream was switched to syngas. After reaction for 1 h the gases were collected (20 min). A sample from the trap, after warming up, was analyzed using GC−MS, and a sample (250 μL) was also taken directly from the reactor outlet at this time for GC analysis. These data are referred to as "before" ethene addition.

After 2.5 h under a syngas stream, 250 μL of labeled ethene ($^{13}C_2H_4$) was injected into the syngas stream via a septum at the reactor inlet and low-temperature collection was started. Labeled ethene was injected every 5 min for 50 min, and the products were collected at −197 °C. This long collection time was needed to obtain sufficient product concentration for ^{13}C NMR spectroscopy and GC−MS analysis.

A sample of the product stream (250 μL) was taken for GC analysis at 21 min after the first ethene injection (1 min after the fifth injection). After the final injection the cold trap was removed and warmed. A sample from the trap was analyzed using GC−MS. These GC and GC−MS product analyses ("snapshots") are referred to as "during" ethene addition. The reaction products from the trap were also analyzed by ^{13}C NMR spectroscopy.

A final sampling for GC analysis was performed at 2 h after the final ethene injection, and subsequently the syngas stream was replaced by hydrogen. The final GC analysis is referred to as "after" ethene

(41) Attempts to use mass spectrometry to define the positions of ^{13}C atoms in labeled long-chain hydrocarbons failed due to the complex and unpredictable fragmentation processes that these molecules undergo in the mass spectrometer.

(42) The elucidation of mechanistic information for a heterogeneously catalyzed reaction by adding a labeled probe molecule to the reactants and then analyzing for the labels in the products is a well-established and widely used technique. It is based on the principle that if the probe resembles an active species in the reaction under investigation, incorporation of the probe will occur. It has the advantage in that it does not depend on identifying very small amounts of labile and highly reactive species on surfaces that are themselves changing and difficult to characterize.

(43) "*Mild conditions*" are defined as 1 atm pressure, CO:H_2 = 1:1, and operating temperatures of Ru/150 °C, Co/180 °C, Rh/190 °C, and Fe/220 °C, which were the lowest that gave reasonable amounts of products (especially for ^{13}C NMR analysis) on the equipment within useful time scales.

(44) Dilabeled ethene ($^{13}C_2H_4$) was used in preference to the more conventional monolabeled probe; this allowed the investigation of C−C cleavage as well as C−C formation reactions.

(45) The amounts of ethene probe added with respect to converted CO were kept as low as possible (1:∼6) in order not to perturb the system excessively, but where the activity was low and it was difficult to accumulate sufficient material for the ^{13}C NMR analysis, a higher proportion of ethene was used.

Table 1. Product Formation Rates (pfr's, μmol/g/h) of 1-Alkenes, Alkanes, Internal Alkenes, and Methane Produced over Ru, Co, Rh, and Fe, before and during $^{13}C_2H_4$ Probe Addition

	Ru/150 °C		Ru/165 °C		Ru/180 °C	
	pfr's before[a]	pfr's during[b]	pfr's before[a]	pfr's during[b]	pfr's before[a]	pfr's during[b]
products						
1-alkenes	100	774	331	1482	503	645
alkanes	31	196	106	997	197	771
2-alkenes	13.5	14	50	84	95.5	87
methane	35	22	127	88	256	116
total activity[c]	199		707		1192	
CO conversion (%)	1.5		5		8	
α[d]	0.68	0.55	0.70	0.56	0.69	0.53

	Co/180 °C		Co/200 °C		Co/220 °C	
	pfr's before[a]	pfr's during[b]	pfr's before[a]	pfr's during[b]	pfr's before[a]	pfr's during[b]
products:						
1-alkenes	100	667	320	495	827	992
alkanes	46	1022	269	1161	1055	1540
2-alkenes	19	47	114	190	439	526
methane	93	83	318	364	1242	1369
total activity[c]	317		1163		3816	
CO conversion (%)	2.4		9		30	
α[d]	0.73	0.72	0.65	0.68	0.53	0.56

	Rh/190 °C		Fe/220 °C	
	pfr's before[a]	pfr's during[b]	pfr's before[a]	pfr's during[b]
products:				
1-alkenes	67	104	137	248
alkanes	36	261	80	334
2-alkenes	28	39	61	55
methane	120	116	155	76
total activity[c]	291		438	
CO conversion (%)	3.2		4.1	
α[d]	0.47	0.43	0.43	0.39

[a] pfr's (product formation rates, μmol/g-cat/h) before probe addition. [b] A snapshot of the pfr's (μmol/g/h) during probe addition. [c] Total pfr's (μmol/g-cat/h including oxygenates and $C_{\geq 7}$) before probe addition. [d] α = chain growth probability.

addition. Further data and product formation rates (Supporting Information) were used for calculating α (listed in Tables 1 and 2).

Analytical Instrumentation. Quantitative analysis of the reaction products was carried out on a Perkin-Elmer Autosystem XL GC fitted with a Supelco SPB-1 column (60 m × 0.53 mm × 5 μm) and a flame ionization detector. The detector was precalibrated with external standards of known concentration. ^{13}C incorporation was analyzed using a Hewlett-Packard 5890−5971A GC−MS fitted with an electron-impact ion source, a hyperbolic quadrupole mass filter, and an electron multiplier detector. C_4-C_7 hydrocarbons were separated on the Supelco SPB-1 column, and C_1-C_3 hydrocarbons were separated using a CP−Sil-5 CB column coupled to a Chrompack PLOT alumina column (30 m × 0.32 mm).[46]

^{13}C NMR Spectra. To obtain sufficient sample for ^{13}C NMR analysis, the products obtained during the $^{13}C_2H_4$ addition into the F−T reaction were collected in a liquid nitrogen trap and sampled by GC−MS. The cold trap containing the condensed F−T products was reimmersed in liquid nitrogen, deuteriochloroform (1 cm^3, Aldrich) was added, and the trap was transferred into a dry ice/acetone bath. The trap was occasionally removed from the cold bath and shaken to ensure that the contents were mixed before transferring them into an NMR tube to record the spectrum. The ^{13}C NMR spectra were measured at 100.6 MHz on a Bruker AMX2-400 using a 5 mm standard geometry

(46) Good GC separations and quantifications were obtained for the hydrocarbons, except for propene, propane, and those with eight or more carbon atoms.

Table 2. Product Formation Rates (pfr's, μmol/g/h) of 1-Alkenes, Alkanes, and 2-Alkenes for Each of C_2, C_3, C_4, C_5, C_6, and C_7 at Different Syngas Flow Rates over Ru at 160 °C (no probes added)

	pfr's (μmol/g/h)		
	450 cm^3/h	900 cm^3/h	1800 cm^3/h
products:			
methane	57	67	90
ethene	1.4	2.3	4.1
ethane	2.8	2.6	2.9
propene	11	11	13.6
propane	1.7	1.7	1.6
1-butene	7.6	8.4	11
butane	3.1	2.6	2.7
2-butenes	1.1	1.6	1.5
1-pentene	3.5	4	5.7
pentane	2.3	1.8	1.9
2-pentenes	1.7	1.6	1.4
1-hexene	1.3	1.5	2.5
hexane	1.8	1.5	1.5
2-hexenes	1.6	1.6	1.5
1-heptene	0.5	0.6	1.1
heptane	1.3	1.1	1.2
2-heptenes	1	1	1.1
CO conversion (%)	3.6	2.1	1.3
chain growth (α)	0.63	0.63	0.63

VSP probe and the following parameters: sweep width 184 ppm, 30° pulse, 4 s relaxation delay, 128K time domain, and 64K frequency domain data points.

The ^{13}C NMR spectra were run under conditions chosen to produce a good signal-to-noise ratio. The signals due to the CH, CH_2, and CH_3 groups showed marked differences in intensity, and ^{13}C NMR intensities were only used to determine relative concentrations of isotopomers within a given signal. Assuming that the relaxation is exclusively dipole−dipole, then the ratio of T_1 for a $^{13}CH{=}{}^{12}\mathbf{C}$ group: $^{13}CH{=}{}^{13}\mathbf{C}$ group is 1.02:1.00. This will also reduce the NOE by a similar amount. The combination could result in a reduction in magnitude of the intensity of the $^{13}\mathbf{C}H{=}{}^{13}C$ signal by up to 5%, an error comparable with that due to the signal-to-noise ratio. The presence of other relaxation mechanisms, the longer $^{13}C(sp^3)-{}^{13}C(sp^3)$ or $^{13}C(sp^2)-{}^{13}C(sp^3)$ bond length, and/or the presence of two ^1H in a CH_2 group reduce this possible error.

Since many of the ^{13}C resonances of the individual hydrocarbons had closely similar chemical shifts, accurate shift determinations were vital. To do this the ^{13}C NMR spectra of pure commercial samples of more than 25 individual hydrocarbons (up to C_7), as well as of some oxygenates that either had been found (by GC−MS) or which had been reported by others to occur in the products, were carefully recorded in $CDCl_3$. To ensure good matches, conditions as near as possible to those used in recording the spectra of the F−T reaction products were used. The agreement with the reference spectra (listed in the Supporting Information) was very good; the small differences (0.01−0.02 ppm) that are seen arise from isotope shifts in the doubly labeled compounds.

The ^{13}C NMR spectrum of an unenriched pure hydrocarbon consists of only single peaks due to the different carbon atoms in the hydrocarbon molecule, since the probability of two ^{13}C atoms being next to each other (and coupling) is negligibly low (0.01%). By contrast, the ^{13}C NMR spectrum of the hydrocarbon mixture produced during the $^{13}C_2H_4$ addition showed multiplets indicating di- and poly-^{13}C incorporation into the products. On the basis of the chemical shifts, multiplicities, and couplings, the compound present, as well as the positions of the ^{13}C nuclei in the hydrocarbon chains, can be determined. The multiplet peaks can be readily identified by their specific carbon−carbon coupling constants: $^1J_{(C-C)}$ (sp^3-sp^3) ∼ 34.5 Hz; $^1J_{(C-C)}$ (sp^3-sp^2) ∼ 42 Hz, while $^1J_{(C-C)}$ (sp^2-sp^2) ∼ 69 Hz.[47] The couplings between two carbons separated by more than one bond are very small, for example in 1-butene, $^3J_{1-4} = 4$ Hz, $^2J_{2-4} = 2$ Hz, and $^2J_{1-3} = 0$.

The resonances for all the carbon atoms of propene and 1-butene, the observed products formed in greatest amount, are well-separated

Table 3. Comparison of Thermodynamic (Calculated) Ratios for Isomeric Butenes and the Experimental Values, during F−T Reactions, over Ru, Co, Rh, and Fe (before and during the Addition of $^{13}C_2H_4$ Probes)

catalyst/ temp, °C	notes	ratio		
		1-butene	*trans*-2-butene	*cis*-2-butene
Ru/180	calculated	1	5	3
	before probe addition	1	0.04	0.1
	during probe addition	1	0.04	0.3
Co/200	calculated	1	5	3
	before probe addition	1	0.2	0.2
	during probe addition	1	0.15	0.2
Co/220	calculated	1	4	2.5
	before probe addition	1	0.5	0.5
	during probe addition	1	0.5	0.4
Fe/220	calculated	1	4	2.5
	before probe addition	1	1.4	1
	during probe addition	1	1.3	1
Rh/190	calculated	1	5	3
	before probe addition	1	0.9	0.7
	during probe addition	1	0.6	0.6

from resonances of other hydrocarbons; thus, their spectra were fully analyzed. The ^{13}C resonances of the CH_3 groups of most of the linear hydrocarbons with more than four carbon atoms formed in the F−T reaction lie in the region δ 13.2−14.5, and those of the adjacent $-CH_2-$ are between δ 21.8 and 23.0, and these resonances were assigned for linear alkanes and alkenes up to C_6. Only for the reactions over Rh was there any sign of branched chain hydrocarbons in the products. Correlating the NMR and the GC−MS data also added considerable confidence to the assignment of resonances.

Results

Product Formation Rates over Co, Ru, Rh and Fe (No Probes Added). The product formation rates (pfr's) for the F−T active metal catalysts under *mild conditions* (columns "pfr's before") listed in Table 1 (Ru, Co, Rh and Fe) show that, in the absence of probe molecules, the products were very similar and comprised linear 1-alkenes, alkanes, internal alkenes, and methane.[48] Although the activities and the exact ratios of the hydrocarbons formed depended on the metal, the nature of promoters (if any), and particularly on the reaction temperature,[49] 1-*n*-alkenes were always major products. Rh and Fe were better catalysts for methanation than Fischer−Tropsch, and methanation was important for cobalt, especially at higher temperatures, where alkanes also became more significant products than 1-alkenes. Changes in the pfr's with changes in temperature (over Ru and Co, Table 1) and syngas flow rates (over Ru, Table 2) were monitored, but it was impracticable to investigate the effects of changes in flow rate or temperature over the Fe and Rh catalysts. It may be noted that the proportion of the thermodynamically favored 2-alkenes was rather higher and significantly closer to the expected equilibrium values from reactions over Fe and Rh than over Ru or Co. Thermodynamic ratios calculated for the isomeric butenes[50] are compared with the experimental values in Table 3.[51]

Reactions with $^{13}C_2H_4$ Probes: GC and GC−MS Data. The responses to the addition of $^{13}C_2H_4$ probes to ongoing F−T reactions carried out over the four catalysts under mild conditions were basically very similar[52] (Table 1 and Supporting Information): (i) methane formation decreased over Ru, Rh, Fe, and over Co at 180 °C; (ii) the 1-alkene, internal alkene, and alkane pfr's increased substantially during probe addition over Co and Ru (at 150 and 165 °C)[53] but then dropped afterward, frequently below the value before probe addition; (iii) a substantial proportion of the hydrocarbon products contained two ^{13}C atoms, while the $^{13}C_1$ and $^{13}C_3$ incorporations were very small and close to natural abundances (by MS analysis). In addition, the internal alkenes (especially the 2-butenes) contained significant amounts of $^{13}C_4$; these must arise from the coupling of two $^{13}C_2H_4$ probes.[54]

Increasing temperature *decreased* the observed $^{13}C_2$ incorporations because, although there was an increase in catalyst activity, as the same amount of probe had been added to each experiment, the increase in ^{12}CO conversion was not balanced by an increase in $^{13}C_2H_4$. This is also shown by the increase in unlabeled products that dilute the $^{13}C_2$-hydrocarbons. The $^{13}C_2$ incorporation also decreased as the molecular weights of the hydrocarbons increased.[55,56] At higher temperature (180 °C/Ru), the incorporation of $^{13}C_1$ increased more than expected from ^{13}C natural abundance, and $^{13}C_3$ also increased significantly.

Table 4 lists the ratios of $^{13}C_n$ incorporation derived from MS data in C_4 hydrocarbons produced over cobalt. Even at the comparatively low reaction temperatures of 180 °C over cobalt (and 150 °C over ruthenium, Supporting Information), the levels of $^{13}C_1$ incorporations were above those expected from natural abundance $^{13}C_1$, indicating that significant probe cleavage had occurred, the amounts of which increased at higher temperatures. This was confirmed by the ^{13}C NMR analysis.

The levels of $^{13}C_2$ incorporated into the hydrocarbon products decrease with increasing temperature. This decrease is due to the decrease in the ratio of $^{13}C_2H_4$ to converted CO with increasing CO conversion and to probe cleavage at higher temperatures. If probe cleavage remained constant with increasing temperature, then the level of $^{13}C_1$ incorporation should decrease in a similar fashion. However, the level of $^{13}C_1$ remains approximately constant or increases with increasing temperature. The contribution of probe cleavage to the level of $^{13}C_1$ incorporation is indicated by the increase in the $^{13}C_1{}^*/^{13}C_2$ ratio (Table 4), where $^{13}C_1{}^*$ is the corrected $^{13}C_1$ incorporation. The ratio $^{13}C_1{}^*/^{13}C_2$ increases significantly with temperature, dem-

(47) Marshall, J. L. *Carbon−carbon and carbon-proton NMR couplings*; Verlag Chemie International: Deerfield Beach, FL, 1983.
(48) Fischer−Tropsch reactions also give oxygenates (methanol, ethanol, ethanal, ethanoic acid, etc.) but in very small amounts (typically ca. 1−3% of the 1-alkenes) over Ru, Co, and Fe. Even smaller amounts of branched-chain hydrocarbons (methylbutenes and -pentenes, ≪1%) were also found. Over the Rh−CeO_n catalysts oxygenates became significant products and smaller amounts of the higher hydrocarbons were formed. As only very minor amounts of these compounds were produced in the reactions reported here, they will be considered in a later paper.
(49) Pressure and the ratio of H_2:CO were less significant variables and were only briefly examined in this work.
(50) Weast, R. C., Ed., *Handbook of Chemistry and Physics*, 1st student ed.; CRC Press: Cleveland, OH, 1988.
(51) The numbers for the pentene and hexene isomers are given in the Supporting Information.
(52) The main differences were that over Rh−CeO_n less $^{13}C_2$ incorporation was found in the 1-*n*-alkenes than in the *n*-alkanes or 2-*n*-alkenes and that the increase in pfr's during ethene addition over Fe at 220 °C was masked by catalyst deactivation.
(53) Smaller changes in pfr's were found over the other catalysts on addition of the probe.
(54) 2-Methyl-2-butene also contained significant amounts of $^{13}C_4$ (by GC−MS), but this was a very minor product (∼0.1% of the total hydrocarbons).
(55) Raje, A.; Davis, B. H. *R. Soc. Chem. Specialist Periodical Rep. "Catalysis"* **1996**, *12*, 52.
(56) In order not to swamp the Fischer−Tropsch reaction with an excess of probe added in one single large tranche, the ^{13}C-labeled probe molecule was added in equal smaller portions over a given period of time in the experiments. The proportions of the various ^{13}C isotopomers found by MS analysis of the products are reproducible from one experiment to another. However, calculation of the expected isotope ratios in the various products is more complicated than originally allowed for. Such a full and detailed evaluation has not yet been attempted and we are therefore not including a kinetic analysis here.

Table 4. Ratios of $^{13}C_n$ Incorporation in C_4 Hydrocarbons Produced from CO + H_2 + $^{13}C_2H_4$ over Cobalt at 180, 200, and 220 °C from MS Data[a]

	$^{13}C_1$ (natural abundance)	$^{13}C_2$	$^{13}C_3$	$^{13}C_4$	$^{13}C_1$*[b]	($^{13}C_1$*/$^{13}C_2$) × 100
1-butene						
180 °C	9 (5)	14	4	1	4	31
200 °C	12 (5)	15	5	3	7	51
220 °C	7 (5)	2	1	1	2	95
butane						
180 °C	10 (5)	23	7	1	5	24
200 °C	11 (5)	16	7	3	6	28
220 °C	11 (5)	6	5	3	6	106
trans-2-butene						
180 °C	12 (5)	28	8	5	8	28
200 °C	14 (5)	23	12	6	7	40
220 °C	10 (5)	6	5	4	5	86
cis-2-butene						
180 °C	13 (5)	27	13	31	8	30
200 °C	14 (5)	22	14	45	9	42
220 °C	10 (5)	6	4	5	5	86

[a] For clarity, the ^{13}C incorporation data obtained from MS analysis were renormalized to $^{13}C_0$ as 100 and were calculated as the ratio of $^{13}C_1$- to $^{13}C_n$-labeled products; the $^{13}C_0$ values are omitted. [b] $^{13}C_1$*, the corrected $^{13}C_1$ incorporation = {$^{13}C_1$(found) − $^{13}C_1$(natural abundance expected)}.

onstrating that probe cleavage increases with temperature, an observation that is not directly evident from the absolute values of $^{13}C_1$ incorporation.

Probe Reactions Using $^{13}C_2H_4$: Product Analysis by ^{13}C NMR Spectroscopy. ^{13}C NMR spectra of the crude products obtained from reactions of $^{12}CO + H_2 + {}^{13}C_2H_4$ (and also other probes) over four metals at different temperatures were measured (Experimental Section). The salient features of the spectra using ethene probes were the pairs of doublets ($^1J_{(C-C)}$ = 34.5 Hz) arising from ^{13}C in *both* the $-CH_3$ (δ 13.3−14.5) and the adjacent $-CH_2-$ (δ 21.8−23.0) in the molecules. This was particularly so for the spectra of products obtained at the lowest temperatures for each metal and indicated that the labels from the $^{13}C_2H_4$ probes appeared mainly in the alkyl tails.

1-Alkene Products: Propene. ^{13}C NMR spectra of the propene produced from reactions under mild conditions showed doublets at δ 19.335 (CH_3) and 133.76 (−CH═) ($^1J_{(C-C)}$ = 42 Hz; Ru at 150 °C, Figure 1a; Co at 180 °C, Figure 2a) as well as at 115.58 (═CH_2) over Rh and Fe (Figure 3c,d). The spectra from reactions over Ru and Co indicated that the propene was almost exclusively $^{13}CH_3{}^{13}CH{=}CH_2$, clearly illustrated by the doublet central −*C*H═ resonance. By contrast, the ^{13}C NMR spectra of the propene formed over rhodium at 190 °C and over iron at 220 °C showed *two* doublets for the central ═CH− at δ 133.76 with ^1J = 42 and 69 Hz arising from coupling to *both* the methyl *and* to the vinylic ═CH_2 (doublet at δ 115.54, ^1J = 69 Hz; Figure 3c,d), indicating that two isotopomers of propene-$^{13}C_2$ ($^{13}CH_3{}^{13}CH{=}CH_2$ and $CH_3{}^{13}CH{=}{}^{13}CH_2$, of approximately equal intensities) had been formed.[57] The NMR spectra showed that Ru and Co gave only very small amounts of $CH_3{}^{13}CH{=}{}^{13}CH_2$. Additional peaks, especially in the higher temperature reaction products (Figures 1c and 2c), indicate the formation of the three monolabeled propenes, $^{13}CH_3$-$CH{=}CH_2$, $CH_3{}^{13}CH{=}CH_2$, and $CH_3CH{=}{}^{13}CH_2$ (singlets at δ 19.335, 115.54, and 133.76), together with some trilabeled propene $^{13}CH_3{}^{13}CH{=}{}^{13}CH_2$.

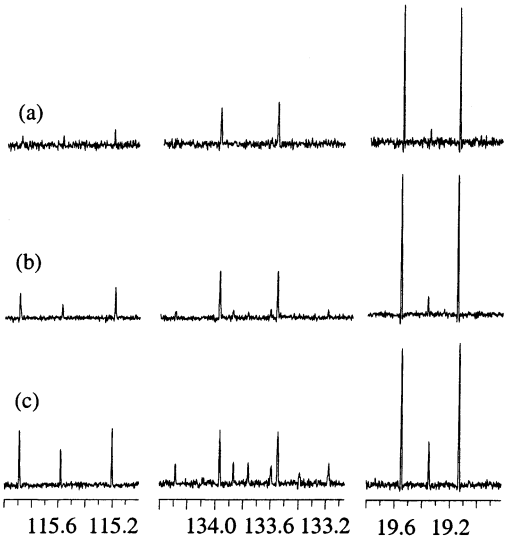

Figure 1. ^{13}C NMR spectrum of propene from $^{12}CO + H_2 + {}^{13}C_2H_4$ over Ru at 150 °C (a), 165 °C (b), and 180 °C (c), showing the CH_2═ (δ 115.54), ═CH− (δ 133.76), and $-CH_3$ (δ 19.35) resonances

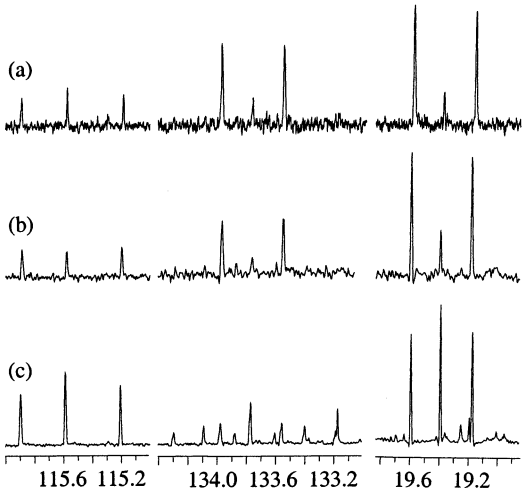

Figure 2. ^{13}C NMR spectrum (δ) of propene from $^{12}CO + H_2 + {}^{13}C_2H_4$ over Co at 180 °C (a), 200 °C (b), and 220 °C (c), showing the CH_2═ (δ 115.54), ═CH− (δ 133.76), and $-CH_3$ (δ 19.35) resonances.

1-Butene. The NMR spectrum of labeled 1-butene (Figure 4a) formed over Ru at 150 °C showed just two doublets (δ 13.05, 26.66, $^1J_{(C-C)}$ = 34.5 Hz), indicating it to be very largely $^{13}CH_3{}^{13}CH_2CH{=}CH_2$. The same isotopomer was formed over Co at 180 °C and over Fe at 220 °C (Figure 4b,d).

As rhodium had a low selectivity toward 1-alkene formation, the resonances for 1-butene were weak; however, doublets at δ 13.05 and 26.66 (Figure 4c) indicated the presence of some $^{13}CH_3{}^{13}CH_2CH{=}CH_2$. The spectra from the higher temperature reactions over Ru and over Co were similar and showed the presence of all four monolabeled butenes (1-butene-$^{13}C_1$) as well as $^{13}CH_3{}^{13}CH_2{}^{13}CH{=}{}^{13}CH_2$, $^{13}CH_3{}^{13}CH_2{}^{13}CH{=}CH_2$, $^{13}CH_3{}^{13}CH_2$-$CH{=}{}^{13}CH_2$, and $CH_3CH_2{}^{13}CH{=}{}^{13}CH_2$, in addition to $^{13}CH_3{}^{13}CH_2$-$CH{=}CH_2$ (Supporting Information).[58] The ratio of 1-butene-

(57) Experiments were also carried out with CO:H_2 ratios of 1:2. In each case (Ru/150 °C, Co/180 °C, Rh/190 °C, and Fe/220 °C) the spectra of propene and of the higher hydrocarbons were essentially identical to those obtained at a CO:H_2 ratio of 1:1.

(58) The presence of some comparatively weak resonances in the same positions in the 1-butene formed at high-temperature reactions over Co suggests that these other species were also present there but were obscured by the much stronger signals of the mono- and the dilabeled 1-butene isotopomers.

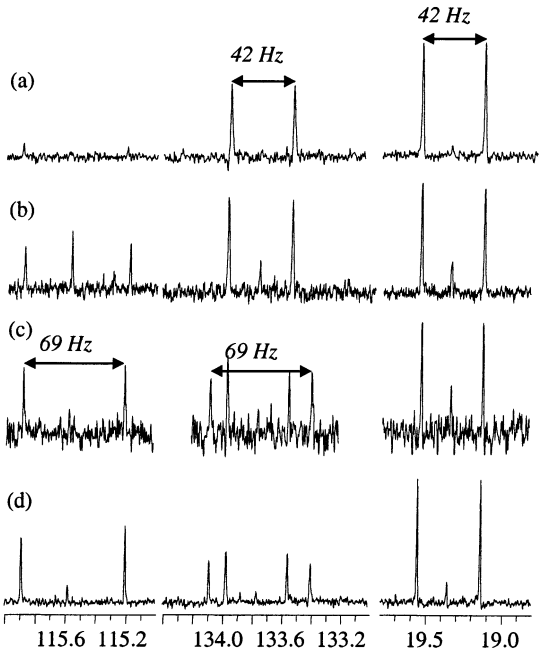

Figure 3. ^{13}C NMR spectra (δ) of propene formed from $^{12}CO + H_2 + {}^{13}C_2H_4$ over (a) ruthenium at 150 °C, (b) cobalt at 180 °C, (c) rhodium at 190 °C, and (d) iron at 220 °C in the $CH_2{=}$, $=CH-$, and $-CH_3$ regions (δ 115.54, 133.76, and 19.35 respectively), showing the presence of $CH_2{=}{}^{13}CH-{}^{13}CH_3$ (^1J = 42 Hz; over Ru, Co) and of $CH_2{=}{}^{13}CH-{}^{13}CH_3$ plus $^{13}CH_2{=}{}^{13}CHCH_3$ (^1J = 69 Hz; over Rh, Fe).

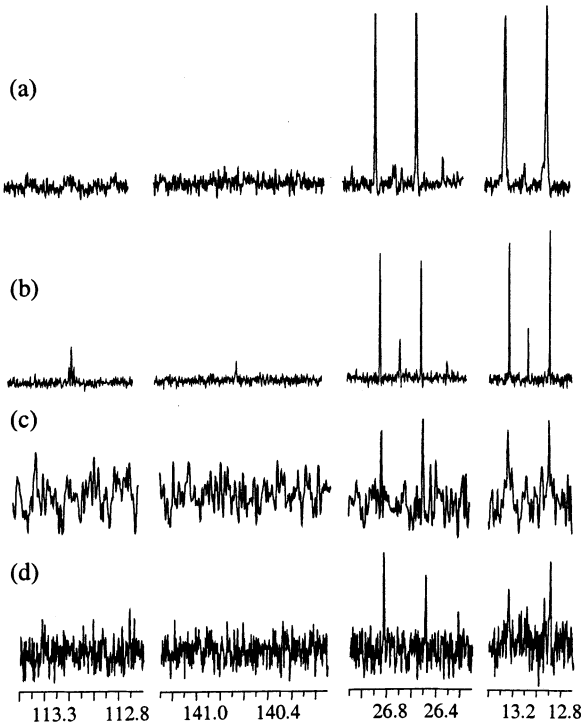

Figure 4. ^{13}C NMR spectra (δ) of 1-butene formed from $^{12}CO + H_2 + {}^{13}C_2H_4$ over (a) ruthenium at 150 °C, (b) cobalt at 180 °C, (c) rhodium at 190 °C, and (d) iron at 220 °C in the $CH_2{=}$, $=CH-$, $-CH_2-$, and $-CH_3$ regions. All show the presence of largely the single isotopomer $CH_2{=}CH{}^{13}CH_2{}^{13}CH_3$.

$^{13}C_1$ to 1-butene-$^{13}C_2$ increased with temperature and, in agreement with the MS data, the 1-butene-$^{13}C_1$ isotopomers were the most conspicuous species from reactions over Co at 220 °C. As the catalyst activity at 220 °C over Co was very high, the amounts of propene and 1-butene produced directly from CO and H_2 were large and thus the $^{13}C_1$ singlets in 1-butene were strong.

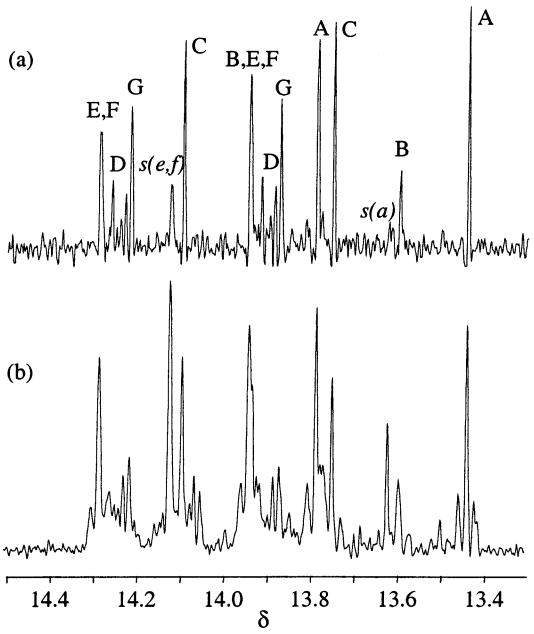

Figure 5. ^{13}C NMR spectra (δ) of higher hydrocarbons in the terminal CH_3 region formed over Ru at 150 °C (a) and at 180 °C (b). The peaks marked A−G are methyl doublets arising from the doubly labeled (A) 1-pentene, (B) butane, (C) 1-hexene, (D) pentane, (E) hexane, (F) heptane, and (G) 1-heptene. The peaks marked *s(x)* are singlets arising from the hydrocarbons containing only one ^{13}C.

1-Pentene, 1-Hexene, and 1-Heptene. The spectra of higher 1-alkenes produced at 150 °C over Ru and over Co at 180 °C showed doublets at δ 13.61 and 22.07, and 13.93 and 22.18 (Figure 5 and Supporting Information), indicating that 1-pentene and 1-hexene were present as $CH_2{=}CHCH_2{}^{13}CH_2{}^{13}CH_3$ and $CH_2{=}CHCH_2CH_2{}^{13}CH_2{}^{13}CH_3$. Although the spectra from the products of the iron and rhodium reactions had poorer signal-to-noise ratios, the pairs of doublets due to $CH_2{=}CHCH_2{}^{13}CH_2{-}{}^{13}CH_3$, $CH_2{=}CHCH_2CH_2{}^{13}CH_2{}^{13}CH_3$, and the *n*-alkanes can be seen. The major peaks from reactions over Co at 220 °C (Figure 6) were singlets due to the monolabeled $^{13}CH_3CH_2CH_2CH{=}CH_2$($\delta$ 13.93) and $CH_3{}^{13}CH_2CH_2CH{=}CH_2$ (δ 22.07), but doublets indicative of dilabeled 1-pentene and 1-hexene were also present, though in relatively small amount.

Comparison of the NMR spectra of the products from reactions over Ru at 180 °C with those of products obtained at 150 °C (Figure 5) showed broadly the same features, namely doublets arising from 1-pentene (at δ 13.61, 22.07; $^1J_{(C-C)}$ = 34.5 Hz), 1-hexene (at δ 14.06, 22.20 $^1J_{(C-C)}$ = 34.5 Hz), as well as *n*-pentane, *n*-hexane, and *n*-heptane. However, the singlets were stronger in the spectra from the higher temperature reaction, indicating more $^{13}C_1$ incorporation. The spectra of products of reactions over Co at 220 °C (Figure 6) showed the presence of both mono- and dilabeled hydrocarbons.

The NMR spectrum of the ^{13}C-labeled 1-pentene formed over Ru at 180 °C (Supporting Information) indicated the presence of $^{13}CH_3{}^{13}CH_2CH_2CH{=}CH_2$ (doublets, $^1J_{(C-C)}$ = 34.1 Hz, centered at δ 13.59 and 22.09), all the five monolabeled 1-pentenes, as well as di-, tri-, tetra-, and even pentalabeled 1-pentene ($^{13}CH_2{=}{}^{13}CH{}^{13}CH_2{}^{13}CH_2{}^{13}CH_3$). The spectra were not sufficiently resolved to allow useful quantification.

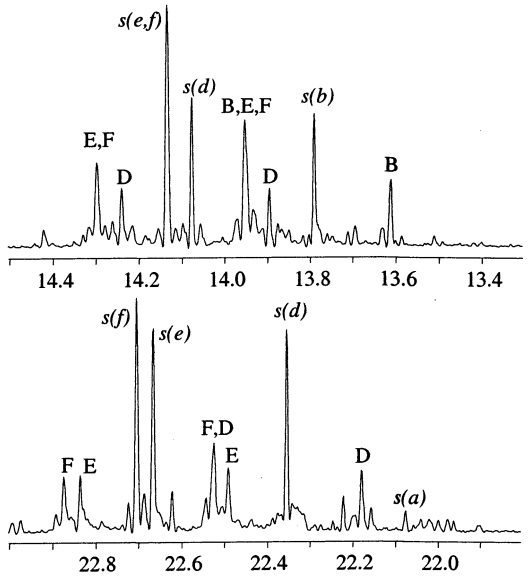

Figure 6. ^{13}C NMR spectrum (δ) of the higher hydrocarbons formed from $^{12}CO + H_2 + {}^{13}C_2H_4$ over cobalt at 220 °C, showing the ethyl regions: $-CH_3-$ (top) and the penultimate $-CH_2-$ (bottom). The peaks marked (B−F) are methyl doublets arising from the doubly labeled $R-{}^{13}CH_2{}^{13}CH_3$: (B) butane, (C) 1-hexene, (D) pentane, (E) hexane, and (F) heptane, while those marked *s(x)* are singlets arising from the monolabeled species $R-CH_2{}^{13}CH_3$ and $R-{}^{13}CH_2CH_3$, respectively.

In the spectrum of the products formed over Ru at 180 °C, a doublet centered at δ 14.045 ($^1J_{(C-C)} = 34.6$ Hz) is assigned to the methyl of 1-*n*-heptene. However, this resonance is weak and the CH_2 to which it is coupled lies directly under the stronger resonances of *n*-pentane and *n*-heptane. Similar peaks are seen in the products from reactions over cobalt and are probably present, though not clearly resolved, in the spectra from reactions over Fe and Rh.

***n*-Alkanes.** In addition to the 1-alkenes, the ^{13}C NMR spectra of the low-temperature reaction products from both cobalt and ruthenium showed strong doublets with $^1J_{(C-C)} = 34$ Hz for the methyls in terminally labeled *n*-butane, *n*-pentane, *n*-hexane, and *n*-heptane, $CH_3(CH_2)_n{}^{13}CH_2{}^{13}CH_3$ (centered at δ 13.76, $n = 1$; 14.06, $n = 2$; 14.12, $n = 3$; and 14.10, $n = 4$). The doublets corresponding to the penultimate CH_2s in these alkanes (at δ 21.84, 22.34, 22.69, and 22.78, respectively) were also clearly visible (Figures 5 and 6). The spectra confirmed the GC−MS data, which indicated the presence of the dilabeled *n*-alkanes, C_nH_{2n+2}. In further amplification of the GC−MS results, the NMR doublets were accompanied by singlets at their mean positions, signifying the presence of the monolabeled $CH_3(CH_2)_n{}^{13}CH_2CH_3$ and $CH_3(CH_2)_nCH_2{}^{13}CH_3$ ($n = 1-4$). The signals were somewhat stronger in the products from the higher temperature reactions (Co at 200 and 220 °C), but no useful quantification was possible.

The main differences between the spectra of the products obtained from the Ru and Co reactions were that the resonances due to the alkane $CH_3(CH_2)_n{}^{13}CH_2CH_3$ and $CH_3(CH_2)_n{}^{13}CH_2{}^{13}CH_3$ carbons were stronger than those for the corresponding alkene-$^{13}C_1$ for Co, whereas the alkene signals were stronger in the Ru products. The products from reactions over Rh/190 °C and Fe/220 °C gave similar patterns, but the $^{13}C_1$-substituted alkanes were noticeably less pronounced.

Internal Alkenes. In the experiments carried out here, the internal alkenes (mainly 2-alkenes, with 2-butenes present in the greatest amount) were significant products (representing 8% of total pfr's for Ru/180 °C, 11% for Co/220 °C, 21% for Fe/220 °C, and 10% for Rh/190 °C; Table 1 and Supporting Information). The NMR data indicate that in the presence of $^{13}C_2H_4$ the *cis*-2-butene formed over Ru/180 °C contained largely $^{13}CH_3{}^{13}CH{=}{}^{13}CH{}^{13}CH_3$[59] and $^{13}CH_3{}^{13}CH{=}CHCH_3$ (Figure 7, ratio ca. 10:1) while *cis*-2-butene formed over Co/220 °C contained $^{13}CH_3{}^{13}CH{=}{}^{13}CH{}^{13}CH_3$, $^{13}CH_3{}^{13}CH{=}CHCH_3$, $^{13}CH_3CH{=}CHCH_3$, $CH_3{}^{13}CH{=}CHCH_3$, and possibly one other polylabeled species (all in about equal amounts). *trans*-2-Butene was also formed in the Co experiment and had similar labeling to the cis; no *trans*-2-butene was seen over Ru. The $^{13}C_4$-labeled 2-butene must arise from a probe dimerization, and we deduce that this occurs stereospecifically (giving only *cis*-2-butene) over Ru.

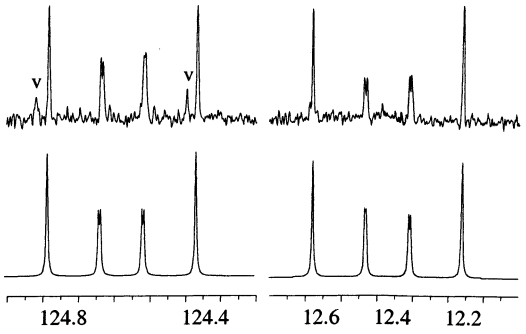

Figure 7. Comparison of the experimental (top) and simulated AA′XX′ (bottom) ^{13}C NMR spectra of *cis*-2-butene-$^{13}C_4$ formed from $^{12}CO + H_2 + {}^{13}C_2H_4$ over ruthenium at 180 °C in the $=CH-$ (δ 124.6) and $-CH_3$ (δ 12.4) regions. [The peaks marked "V" arise from *cis*-2-butene-$^{13}C_2$].

Both *cis*- and *trans*-$^{13}CH_3{}^{13}CH{=}CHCH_3$ were also found in the experiment over Fe/220 °C. Although small amounts of the tetralabeled species are seen in the MS, none is apparent in the NMR; thus, probe dimerization occurred to a negligible extent over Fe. A similar situation was found over Rh.

$^{13}C_1$ Incorporation from Natural Abundance and Probe Cleavage; Quantification of Isotopomer Ratios. The ^{13}C NMR spectra of the crude reaction products from F−T experiments without any labeled probe (Supporting Information) showed a large number of weak singlets arising from the natural abundance ^{13}C in the ^{12}CO used. The strongest resonances in the products formed over Ru/180 °C and Co/220 °C corresponded to the lower *n*-alkanes and 1-alkenes (up to $\sim C_7$), and the assignable peak positions were consistent with the hydrocarbons being randomly labeled with single ^{13}C's in all positions.

The $^{13}C_1$ incorporation found during experiments with labeled probes arose both from probe cleavage and from natural abundance ^{13}C in the ^{12}CO used. At higher temperatures the catalyst activity and hence the conversion of CO increased; thus, more hydrocarbons formed solely from CO and H_2 were collected over the sampling period for the NMR spectra, accounting for the increased intensities from natural abundance $^{13}C_1$.

The relative amounts of the individual $^{13}C_n$ isotopomers in propene and 1-butene (Table 5) were determined by simulating

(59) The ^{13}C NMR spectrum of $^{13}C_4$-labeled *cis*-but-2-ene was simulated by WinDaisy and analyzed as an AA′XX′ spin system. The best match to the experimental spectrum was obtained for a simulated spectrum with four different coupling constants, $^1J_{sp^3-sp^2} = 42.8$, $^1J_{sp^2-sp^2} = 71$, $^3J_{sp^3-sp^3} = 3.7$, and $^2J_{sp^3-sp^2} = -0.7$ Hz. The coupling constants are close to those found for 1-butene and 1-pentene.

Table 5. Isotopomer Abundances in Propene and 1-Butene from CO Hydrogenation over Ru/150 °C, Estimated from WinDaisy Simulation of the ^{13}C NMR Spectra (C* = ^{13}C)

	isotopomer abundance (%) at various propene temperatures			
isotopomer	150 °C	160 °C	165 °C	180 °C
C*═CC	2	3	4	10
C═C*C	2	4	4	7
C═CC*	4	5	6	10
C*═C*C				7
C═C*C*	83	65	67	39
C*═C*C*	8	23	19	27

	isotopomer abundance (%) at various 1-butene temperatures			
isotopomer	150 °C	160 °C	165 °C	180 °C
C*═CCC		4	3	8
C═C*CC		4	4	5
C═CC*C		5	5	8
C═CCC*		5	5	8
C═CC*C*		51	51	31
C*═C*CC		1	2	2
C*═CC*C*		8	7	8
C═C*C*C*		8	9	8
C*═C*C*C*		18	14	22

Table 6. Comparison of Isotopomer Abundances Derived from NMR and MS Analysis

	isotopomer abundance (%) at various temperatures					
	150 °C		165 °C		180 °C	
compd	NMR	MS	NMR	MS	NMR	MS
propene						
propene-$^{13}C_1$	8	8	14	11	26	9
propene-$^{13}C_2$	83	83	67	74	47	63
propene-$^{13}C_3$	8	9	19	15	27	28
1-butene						
1-butene-$^{13}C_1$		13	17	12	27	25
1-butene-$^{13}C_2$		66	53	51	34	33
1-butene-$^{13}C_3$		11	16	18	16	19
1-butene-$^{13}C_4$		11	14	18	23	22

the multiplets observed for each carbon signal. Using WinDaisy software it was possible to obtain very good matches to the experimental spectra when the signals for the isotopomers were sufficiently intense. The WinDaisy simulated spectra of propene matched well with the experimental plots for the Ru-catalyzed reactions, and the isotopomer ratios were in good agreement with those from the MS data from reactions over Ru at 150 and 165 °C, as shown in Table 6.[60,61]

The agreement between the results from the ^{13}C NMR and the mass spectrometry of 1-butene was excellent at all temperatures where it was possible to make measurements. The spectrum of 1-butene formed at 180 °C over ruthenium was used for the calculation of the isotopomer proportions. A WinDaisy-simulated spectrum of the 1-butene isotopomers, close to the one obtained experimentally (Supporting Information), consists of 1-butene labeled $^{13}C_1$ 27%, $^{13}C_2$ 34%, $^{13}C_3$ 16%, and $^{13}C_4$ 23% (Table 6). This composition is in excellent agreement with the MS data, which showed 1-butene-labeled $^{13}C_1$ 25%, $^{13}C_2$ 33%, $^{13}C_3$ 19%, and $^{13}C_4$ 22%, respectively. Thus, the ^{13}C NMR analysis confirms the MS analysis for calculation of the ^{13}C incorporations.

The proportion of $^{13}C_1$ from natural abundance to that from probe cleavage was also estimated by comparing the ^{13}C NMR spectrum of 1-butene formed in the reaction without probe addition to the spectrum of the 1-butene formed during the addition of $^{13}C_2H_4$, both spectra being recorded with the same number of scans and processed with the same parameters. The intensities of the spectra were normalized to the solvent signal, and thus, the contribution of $^{13}C_1$ from the probe was derived from the difference in intensities of the singlets from the two experiments. From the ^{13}C NMR spectra the intensity ratio of $^{13}C_1$ arising from natural abundance plus probe cleavage to the $^{13}C_1$ arising solely from the natural abundance is 2:1. The ratio obtained from the MS data is 3:1, which is the ratio of normalized $^{13}C_1$ to that expected from natural abundance ($^{13}C_1$:$^{13}C_1$*). This implies that $^{13}C_1$ derived from the added $^{13}C_2H_4$ contributed between one-half and two-thirds of the singlet peak intensities of the ^{13}C NMR spectrum of 1-butene.

The same analysis for 1-butene produced in F−T reactions with and without probe addition over cobalt at 220 °C gave a ratio close to 1.5:1 both from the ^{13}C NMR analysis and the MS data. This indicates that over cobalt approximately one-third of the $^{13}C_1$ is derived from the probe and that probe cleavage is more significant for Ru at 180 °C than for Co at 220 °C.

Other Probe Reactions: Nitromethane-^{13}C. The hypothesis that CH_2 is involved in chain growth is supported by studies carried out in which ^{13}C-labeled nitromethane probes were added to a F−T reaction.[27] Adding $^{13}CH_3NO_2$ probe to the syngas stream over cobalt at 180 °C or iron at 220 °C gave considerable and random incorporation of $^{13}C_n$ (Supporting Information).[62] These results confirm that the CH_2 from nitromethane can act similarly to CO in propagating the F−T reaction.

***n*-Propanol.** Although small amounts of oxygenates were formed over all the catalysts tested, only rhodium produced appreciable quantities of methanol, ethanal, ethanol, as well as some *n*-propanol during $^{13}C_2H_4$ probe addition. Mass spectrometry showed that the *n*-propanol was doubly labeled and therefore arose by ethene hydroformylation.

In a further labeling experiment, *n*-propanol-$^{13}C_1$ was added to a CO hydrogenation over the rhodium catalyst. MS analysis of the propene produced showed that no label had been incorporated, nor was there any ^{13}C in any of the normal F−T products. However, the propanol did take part in the reaction, as shown by the formation of 2-methyl-2-butene, which contained 64% $^{13}C_1$. This experiment shows that *n*-propanol was incorporated into branched products but that it was not intermediate in the formation of propene or other linear hydrocarbons.[63]

(60) In this work it was not possible to distinguish the $^{13}C═C^{13}C$ isotopomer of propene from a mixture of $^{13}C═CC$ and $C═C^{13}C$ or the $^{13}C═C^{13}CC$ isotopomer of 1-butene from $^{13}C═CCC$ and $C═C^{13}CC$, as the $^2J \sim 0$. The abundance of these $^{13}C_2$ isotopomers is expected to be low at low reaction temperatures, but they may be significant in higher temperature reactions, as indicated by the data of Percy and Walter (vide infra).

(61) However, the agreement for the 180 °C reaction was poor, and the simulated NMR spectrum isotopomer proportions (propene 26% $^{13}C_1$, 47% $^{13}C_2$ and 27% $^{13}C_3$ propene) did not compare well with the GC−MS data (propene 9% $^{13}C_1$, 63% $^{13}C_2$, and 28% $^{13}C_3$). This discrepancy is ascribed to poor separation of propene and propane in the GC, leading to the molecular ion peak in the GC−MS of *all-*^{12}C-propane interfering with that of $^{13}C_2$-propene, as both have the same *m*/*z* 44 amu. Thus, the proportion of $^{13}C_2$-propene given by the MS analysis is higher than its true value. As less propane was formed at lower reaction temperatures, the peak overlap was smaller, giving much better agreement between the MS and NMR results.

(62) We found nitromethane was more convenient to use than diazomethane as a probe molecule and it gave more consistent results.

(63) See also: van der Riet, M.; Copperthwaite, R G.; Hutchings, G. J. *J. Chem. Soc., Faraday Trans. 1* **1987**, *83*, 2963. Hutchings, G. J.; van der Riet, M.; Hunter, R. *J. Chem. Soc., Faraday Trans. 1* **1989**, *85*, 2875.

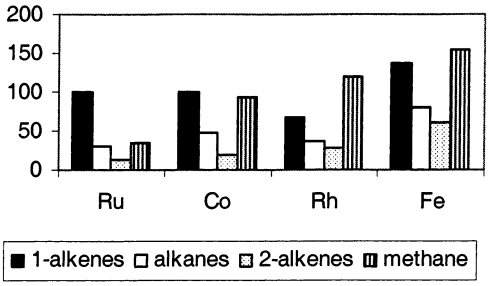

Figure 8. Product formation rates (μmol/g/h) found for CO + H_2 over Ru/150 °C, Co/180 °C, Rh/190 °C, and Fe/220 °C (CO:H_2 1:1, 1 atm, mild conditions); no probes added.

Discussion

F−T Reactions at Lower Temperatures (No Added Probes). Table 1 and Figure 8 (and Supporting Information) show that, while the activities and selectivities varied with metal and temperature, all four of the catalysts used gave basically similar product distributions of linear alkenes, alkanes, and methane from CO hydrogenation under *mild conditions*.[43]

1-Alkenes predominated, but alkanes became more significant among the higher hydrocarbons, while internal olefins (chiefly 2-alkenes) were generally minor products. Methane was often the major single product and its pfr (product formation rate) was closely dependent on the reaction temperature. In agreement with the work of Vannice,[64] Ru was found to be the most active catalyst; however, Co also had high activity for 1-alkene formation.

Table 3 shows that the ratios of internal to terminal alkenes formed in the F−T reactions were much lower than those calculated for thermodynamic equilibrium. For example, at 180−200 °C the products formed over both Ru and Co contain little *cis*- + *trans*-2-butene by comparison to 1-butene (ratios 0.1 and 0.4 respectively, compared to 8 for equilibrium). Over Fe and Rh the ratios (2.4 and 1.6, respectively) were significantly closer to the equilibrium values. This suggests that formation of the internal butenes is largely kinetically determined over Ru and Co but that a significant proportion arise from secondary isomerization processes over Fe and Rh. Further, measurements at different syngas flow rates over Ru (Table 2) show that at lower flow rates proportionately more internal alkenes and alkanes are generally found, while the reverse is true of the 1-alkenes and methane. As *lower* flow rates increase the residence times of the gases on the catalyst, this implies that secondary reactions are involved in the formation of alkanes and 2-alkenes.[65]

F−T Reactions at Lower Temperatures with Added $^{13}C_2H_4$ Probe: Formation of $CH_2{=}^{13}CH^{13}CH_3$ and of $CH_2{=}CH(CH_2)_n{}^{13}CH^{13}CH_3$. Addition of a $^{13}C_2H_4$ probe to the syngas stream over Co, Rh, and over Ru at 150 and 165 °C increased the pfr's of the 1-alkenes and alkanes and to a lesser extent those of the internal alkenes. The methane pfr's decreased over Ru, Rh, and Fe (Supporting Information). Over Ru and Co the pfr's of the 1-alkenes increased substantially up to ca. C_6, but then *n*-alkane formation became more significant.

The objective of this work was a mechanistic study of CO hydrogenation using $^{13}C_2H_4$ probes; thus mild conditions were used[43] such that secondary reactions of the primary hydrocarbon products were minimized. The success with which this was realized can be appreciated from the extremely clean ^{13}C NMR spectra of the crude product mixtures, the analysis of which was relatively straightforward, even though a substantial number of compounds were present. The labeling in the products from incorporation of the $^{13}C_2H_4$ probe was very similar for the various catalysts and featured pairs of doublets ($^1J_{(C-C)} \sim 34.5$ Hz) in the terminal $-CH_3$ (δ 13.2−14.5) and penultimate $-CH_2-$ (δ 21.8−23.0) regions, characteristic of *n*-alkenes and *n*-alkanes with $-{}^{13}CH_2{}^{13}CH_3$ tails. Almost the only other resonances seen elsewhere in the spectra were those of propene (largely $CH_2{=}^{13}CH^{13}CH_3$ from the Co and Ru reactions, plus $^{13}CH_2{=}^{13}CHCH_3$ formed over Fe and Rh), together with some (weak) singlets due to random lone ^{13}C atoms in the hydrocarbons arising from natural abundance ^{13}C in the CO and from some cleavage of the $^{13}C_2H_4$ probe.

The ^{13}C NMR data confirm the MS analysis that the hydrocarbons formed over all the catalysts, under these conditions, contain largely two ^{13}C atoms. Most important, they show that the two ^{13}C atoms are *adjacent to each other in the alkyl terminal positions* of the hydrocarbons, $CH_2{=}CH(CH_2)_n{}^{13}CH_2{}^{13}CH_3$ and $CH_3(CH_2)_{n+1}{}^{13}CH_2{}^{13}CH_3$. There was little evidence for two ^{13}C atoms elsewhere; thus, the initiation is preferentially by a C_2 species, followed by unidirectional chain propagation by a C_1 species.

As there is good correspondence between the NMR, the GC, and the GC−MS data, we are confident that no major organic products ($C_{\geq 7}$) have been missed.[66]

F−T Reactions with Added $^{13}C_2H_4$ Probes at Higher Temperatures. When the $^{13}C_2H_4$ probe F−T reactions were run at higher temperatures, over Co and Ru, the product mix remained similar (by GC) but the NMR spectra became more complex, and a range of isotopomers was formed. In addition to the pairs of doublets signifying the $^{13}C_2$-labeled ethyl tails, clear evidence was found for the incorporation of one, two, three, or four ^{13}C's in individual products; 1-pentene even contained some $^{13}C_5$ isotopomer. In some cases the spectral resolution allowed detailed evaluation of the number of ^{13}C nuclei and of their positions in the various isotopomers.

Comparison with a previous study by Percy and Walter is relevant; they used ^{13}C NMR spectroscopy to analyze the propene formed from CO hydrogenation over cobalt on aluminum at 240 °C using $^{13}C_2H_4$ as probe.[67] Under these higher temperature conditions, very extensive probe cleavage and largely random incorporation of ^{13}C into propene was observed. However, some propenes with two adjacent ^{13}C nuclei were found, which was interpreted to indicate that some ethene was incorporated as a C_2 unit.[68]

(64) Vannice, M. A. *J. Catal.* **1975**, *37*, 449.
(65) Madon, R J.; Reyes, S C.; Iglesia, E. *J. Phys. Chem.* **1991**, *95*, 7795.
(66) However, since the work concentrated on the organic products, CO_2 was not determined.
(67) Percy, L T.; Walter, R I. *J Catal.* **1990**, *121*, 228.
(68) Comparison of the data from our ^{13}C NMR spectra from the reaction over Co−silica (220 °C, 10 mL/min, $^{13}C_2H_4$:CO:H_2 = 1:75:75) with the data obtained by Percy and Walter from a reaction over Co−aluminum (240 °C; 20 mL/min, $^{13}C_2H_4$:CO:H_2 = 1:12:36) shows very similar isotope distribution in the 1-propenes: 1-$^{13}C_1$, ours, 16% (P&W, 14%); 2-$^{13}C_1$, 18 (16); 3-$^{13}C_1$, 22 (14); 1,2-$^{13}C_2$, 13 (15); 2,3-$^{13}C_2$, 16 (17); 1,2,3-$^{13}C_3$, 16 (18). The small differences arise from the different support and the different temperatures. From experiments in which ^{12}CO and $^{13}C_2H_4$, as well as ^{13}CO and $^{12}C_2H_4$, were reacted with H_2 over Co, they were able to estimate that ca. 14% of the propene-$^{13}C_2$ isotopomers had a nonvicinal label, $^{13}CH_3CH{=}^{13}CH_2$. Since we used rather lower reaction temperatures, it is likely that the proportion of $^{13}CH_3CH{=}^{13}CH_2$ in our work was lower still.

F−T Reactions with Other Probes. We also used other C_2 probes in early studies.[18,19,20] Significant increases in the pfr's of the C_3-C_6 hydrocarbons were observed when vinyl bromide ($CH_2{=}CHBr$) was used, indicating substantial probe incorporation in the products. By contrast, addition of an *ethyl* bromide probe to syngas over Ru, Co, Rh, or Fe catalysts caused enhancement only of the product C_2 fraction. Thus although the probe was activated (hydrogenolyzed), no significant incorporation into a Fischer−Tropsch polymerization occurred.[69] For both these probes the catalysts were rapidly deactivated.

$^{13}C_1$ probes were also employed to investigate the reactions. Following the pioneering studies by Wender and co-workers[70] and our own earlier work[71] using nitromethane probes, we also measured ^{13}C NMR spectra of the products obtained on addition of $^{13}CH_3NO_2$ to a CO hydrogenation over Co/220 °C and over Fe/220 °C. These were quite similar to the spectra obtained using a $^{13}C_2H_4$ probe at higher temperatures (e.g., Co/220 °C, Figure 2) and showed random incorporation and random positioning of ^{13}C. For example, the central $-CH{=}$ of propene at δ 133.7 showed the presence of propene-$^{13}C_1$, both propene-$^{13}C_2$, as well as propene-$^{13}C_3$ isotopomers (Figure 1 and Supporting Information), a result which is completely consistent with random mixing of ^{13}C from the probe and ^{12}C from CO.

Mechanistic Considerations. Three aspects to be considered in discussing the mechanism of the formation of *n*-alkenes and *n*-alkanes in the F−T reaction are (i) the nature of the C_1 species, (ii) the involvement of C_2 species as initiators and their likely nature, and (iii) the actual C_1 polymerization and chain termination steps.

C_1 Building Blocks: Chain Propagation with Methylene ($>CH_{2(ad)}$) or with Methylidyne Plus Hydride {$CH_{(ad)} + H_{(ad)}$}. The $C_{1(ad)}$ entity involved in chain growth has usually been formulated as a surface methylene ($>CH_{2(ad)}$) right back to the work of Fischer and Tropsch,[1] and this is supported by a considerable wealth of data from many sources.[3] The existence of $>CH_{2(ad)}$ on metal surfaces relevant to CO hydrogenation reactions has been amply confirmed,[33,72−75] and a number of organometallic reactions involving metal methylene species have been shown to model different aspects of the F−T reaction.[21,31,35−37]

Thus, most authors have discussed mechanisms involving methylene as the propagating monomer; however, recently an alternative proposal has been made, with the polymerization involving sequential methylidyne and hydride {$CH_{(ad)} + H_{(ad)}$} addition. Surface studies, in particular HREELS measured in vacuo at very low temperature, provide good evidence for the formation of $>CH_{2(ad)}$ from diazomethane, CH_2I_2, CH_2ClI, various hydrocarbon precursors (methane, ethene),[72−75] and also CO,[33] on clean surfaces [Ru(0001), Ni(111), Pt(111), Rh(111), etc.]. However, the methylene appears only to be stable below ca. 170 K, and under these conditions decomposition with loss of hydrogen is fast by 200 K and $CH_{(ad)}$ becomes the major species.

The suggestion has thus been made that the $C_{1(ad)}$ propagation in CO hydrogenation could take place in two steps, involving a tri-coordinated methylidyne ($\equiv CH_{(ad)}$) followed by a hydride addition, rather than in a single methylene ($>CH_{2(ad)}$) addition.[76] That proposal has been supported by theoretical considerations recognizing, for example, that CH, CR, and CCH can conveniently sit in a 3-fold surface site, where the carbon is in a low-energy situation coordinated to three metal atoms.

However, the state of $C_{1(ad)}$ on a surface under catalytic conditions *in the presence of hydrogen* (surface hydride) is not clear and needs to be determined first. Organometallic models show that ready interconversions can occur between carbide, methylidyne, methylene, and methyl; for example,

$$[\{Cp(CO)Fe\}_2(\mu\text{-}CO)(\mu\text{-}CH)]^+ + H^- \rightarrow [\{Cp(CO)Fe\}_2(\mu\text{-}CO)(\mu\text{-}CH_2)]$$

$$[\{Cp(CO)Fe\}_2(\mu\text{-}CO)(\mu\text{-}CH_2)] + H^+ \rightarrow [\{Cp(CO)Fe\}_2(\mu\text{-}CO)(\mu\text{-}CH_3)]^+ \quad 77$$

$$[Fe_3C(CO)_{10}]^{2-} + H^+ \rightarrow [Fe_3CH(CO)_{10}]^- \quad 78$$

$$[HOs_3(CO)_{10}CH] + LiBHEt_3 \rightarrow [HOs_3(CO)_{10}(CH_2)]^-$$

$$[HOs_3(CO)_{10}CH_2]^- + H^+ \rightarrow [HOs_3(CO)_{10}CH_3] \quad 79$$

$$Tp^*(CO)_2W{\equiv}C{-}H + RLi \rightarrow Tp^*(CO)_2W{\equiv}C{-}Li + RH \quad 80$$

(Cp = η^5-C_5H_5; Tp* = hydridotris(3,5-dimethylpyrazolylborate))

By analogy to the organometallic chemistry, one would expect there to be ready equilibria between surface species, for example, $CH_{2(ad)} \rightleftharpoons CH_{(ad)} + H_{(ad)}$, in which case the nature of $C_{1(ad)}$ will depend on the equilibrium constant and the concentration of surface hydrogen, which will itself be a function of the hydrogen pressure and the nature of the surface.

The three-coordinate geometry (and the spectrum) of surface CH closely resembles that of the μ_3-methylidyne HC≡ ligand in the known and defined cluster complexes such as (μ_3-RC)-$Co_3(CO)_9$ or (μ_3-RC)$Ru_3(H)_3(CO)_9$ (R = H, alkyl).[81] However, symmetrically bonded μ_3-methylidyne ligands in complexes such as $[(Cp^*)_3Rh_3(\mu_3\text{-}CH)_2]$,[82] are rather inert, and little has so far

(69) Experiments to refine the data further using labeled ethyl bromide are planned.
(70) Cavalcanti, F. A. P.; Oukaci, R.; Wender, I.; Blackmond, D. G. *J. Catal.* **1990**, *123*, 260.
(71) Quyoum, R.; Berdini, V.; Turner, M. L.; Long, H. C.; Maitlis, P. M. *J. Catal.* **1998**, *173*, 355.
(72) Barteau, M. A.; Broughton, J. Q.; Menzel, D. *Appl. Surf. Sci.* **1984**, *19*, 92. Barteau, M. A.; Feulner, P.; Stengl, R.; Broughton, J. Q.; Menzel, D. *J. Catal.* **1985**, *94*, 51. See also Demuth, J. E.; Ibach, H. *Surf. Sci.* **1978**, *78*, L238.
(73) Wu, M.-C.; Goodman, D. W. *J. Am. Chem. Soc.* **1994**, *116*, 1364. CH_3 radicals deposited on Cu(111) behave similarly: Chuang, T. J.; Chan, Y. L.; Chuang, P.; Klauser, R. *J. Electron Spectrosc. Relat. Phenom.* **1999**, *98*−*99*, 149.
(74) Zhou, X. L.; Liu, Z. M.; Kiss, J.; Sloan, D. W.; White, J. M. *J. Am. Chem. Soc.* **1995**, *117*, 3565.
(75) George, P. M.; Avery, N. R.; Weinberg, W. H.; Tebbe, F. N. *J. Am. Chem. Soc.* **1983**, *105*, 1393.
(76) Burghgraef, H.; Jansen, A. P. J.; van Santen, R. A. *J. Chem. Phys.* **1995**, *103*, 6562. Ciobica, I. M.; Frechard, F.; van Santen, R. A.; Kleyn, A. W.; Hafner, J. *Chem. Phys. Lett.* **1999**, *311*, 185. Ciobica, I. M.; Frechard, F.; van Santen, R. A.; Kleyn, A. W.; Hafner, J. *J. Phys. Chem. B* **2000**, *104*, 3364. Ciobica, I. M.; Frechard, F.; Jansen, A. P. J.; van Santen, R. A. *Stud. Surf. Sci. Catal.* **2001**, *133*, 221. Ciobica, I. M. PhD Thesis, Technical University, Eindhoven, 2002.
(77) Casey, C. P.; Fagan, P. J.; Miles, W. H. *J. Am. Chem. Soc.* **1982**, *104*, 1134.
(78) Kolis, J. W.; Holt, E. M.; Drezdzon, M.; Whitmire, K. H.; Shriver, D. F. *J. Am. Chem. Soc.* **1982**, *104*, 6134.
(79) Shapley, J. R.; Cree-Uchiyama, M. E.; St George, G. M.; Churchill, M. R.; Bueno, C. *J. Am. Chem. Soc.* **1983**, *105*, 140.
(80) Enriquez, A. E.; White, P. S.; Templeton, J. L. *J. Am. Chem. Soc.* **2001**, *123*, 4992.
(81) Howard, M. W.; Kettle, S. F. A.; Oxton, I. A.; Powell, D. B.; Sheppard, N.; Skinner, P. *J. Chem. Soc., Faraday Trans. 2* **1981**, *77*, 397. Oxton, I. A. *Spectrochim. Acta A* **1982**, *38*, 181.

been reported on their participation in C−C coupling reactions. By contrast, Knox,[83] Casey,[84] and their collaborators have shown that the μ_2-alkylidynes in the diruthenium and diiron cations *cis*-[{CpRu(CO)}$_2$(μ_2-CO)(μ_2-CMe)]$^+$ and *cis*-[{CpFe(CO)}$_2$-(μ_2-CO)(μ_2-CH)]$^+$ reacted readily with olefins, diazomethane, and other nucleophilic reagents. Shapley et al.[79] also noted similar electrophilic behavior of the "semitriply bridging CH" in [HOs$_3$(CO)$_{10}$CH].

Some congruence has come from surface studies where spectra, assigned to a distorted methylidyne, have been observed from $C_{1(ad)}$ species on Ru(1000) and other metal surfaces, in addition to those of μ_3-CH species.[72] This distorted CH appears to be close to the organometallic μ_2-CH, and if the *catalytically active* $C_{1(ad)}$ is a CH rather than a CH_2, it may be better formulated as μ_2-CH than μ_3-CH. Furthermore, a more labile species should also play a more important role in catalysis than a less reactive one.

Involvement of C_2 Species in the Polymerization. Evidence pointing to the possible involvement of C_2 species in the polymerization process was already found in the very early investigations of the F−T reaction.[5−10] More recently, Mims and McCandlish, monitoring the effects of a switch from labeled to unlabeled CO (isotope transient experiments, without C_2 probe addition) over iron, cobalt, or ruthenium catalysts, suggested that a long-lived C_2 intermediate was a key feature of the reaction to give 1-alkenes.[26,30] The product analysis (by ^{1}H NMR spectroscopy) was interpreted in terms of a C_2-initiated polymerization, with the alkyl termini of the 1-alkene products containing the initiating carbons. The conclusions were very similar to those that we present here based on direct ^{13}C NMR analysis and a doubly labeled ethene probe.

The evidence from our probe data strongly supports initiation by a C_2 species, probably not a surface ethyl, but a surface vinyl ($H_2C{=}CH_{(ad)}$); however, a vinylidene ($CH_2{=}C{=}_{(ad)}$) formulation cannot be excluded.

Routes to 1-Alkenes $CH_2{=}{}^{13}CH^{13}CH_3$ and $CH_2{=}CH(CH_2)_n{}^{13}CH^{13}CH_3$ Based on Propagation by $\{CH_{2(ad)}\}$. Our data indicate that the primary F−T polymerization reaction leads mainly to 1-alkenes; a view shared by most other workers. The ^{13}C NMR spectra showed that 1-alkenes with labeling $^{13}CH_3{}^{13}CH_2(CH_2)_nCH{=}CH_2$ were formed (from ^{12}CO, H_2, and a $^{13}C_2H_4$ probe) over all four metals for $n = 0$, 1, and 2, with good evidence also for $n = 3$, and that the strengths of the signals decreased with increased chain length.

The results from our experiments agree with and significantly expand those derived by Percy and Walter from their NMR work,[67] as well as those from the various isotope transient experiments.[28−30] Since the conclusions from reactions both with and without ethene probe addition are so similar, it confirms that our results relate to CO hydrogenation and not just to reactions of the probe.

Four hypotheses that have been put forward to explain 1-alkene formation based on a polymerization of methylenes $\{CH_{2(ad)}\}$ are (1) the *alkyl* mechanism, where the initiator is a surface hydride and the chain carriers are surface alkyls;[31] (2) the *alkenyl* mechanism, where the initiator is a surface vinyl and the chain carriers are surface alkenyls;[21] (3) the closely related *alkylidene−hydride−alkenyl* mechanism, where the initiators and the chain carriers are surface alkylidenes and alkenyls;[37] and (4) a *metathesis-type* mechanism, where the chain carriers are metallacyclobutanes.[38,85] The experimental data are not in agreement with the alkylidene−hydride−alkenyl or the metathesis-type mechanisms, as the isomers they predict are not formed (Supporting Information).

The alkyl + $\{CH_{2(ad)}\}$ mechanism as originally formulated[31] (Scheme 2) involves sequential reactions of surface alkyls with surface methylenes and starts by reaction of a surface hydride with a methylene; the reaction is terminated by β-elimination of the 1-alkene, $CH_2{=}CHR$, from the alkyl, mCH_2CH_2R. This model has significant shortcomings (Supporting Information), and a number of modifications have been suggested to reconcile the product distribution and labeling data, as follows:[86] the C_2 initiator is needed because initiation requires "special ethyl groups, stabilized by α-CH−m interactions"; the dip at C_2 in the ASF plot arises because ethene π-bonds more strongly to metals than higher olefins; and some methyl-branched minor products arise because of occasional readdition of surface H to an alkene complex. A significant strength of the alkyl mechanism is that it readily explains alkane formation (by hydrogenolysis of the surface alkyl species), *if alkanes are direct F−T products.*

In the alkenyl + $\{CH_{2(ad)}\}$ mechanism (Scheme 3), the chain carrier is a metal−*alkenyl* (M-CH=CHR), and the individual steps are based upon organometallic models. A significant strength is the consideration that alkenyl intermediates in the C−C coupling steps are likely to be much more reactive than metal alkyls.[87−89]

Scheme 4 illustrates the proposed path for $^{13}C_2$ incorporation into 1-alkenes, giving terminally dilabeled 1-butene $CH_2{=}CH^{13}CH_2{}^{13}CH_3$ by an alkenyl + methylene $\{CH_{2(ad)}\}$ mechanism. The ethene ($^{13}C_2H_4$, $^*CH_2{=}{}^*CH_2$) initiator first undergoes C−H activation (top right) to produce a surface vinyl ($^{13}C_2H_{3(ad)}$); organometallic models for this process are plentiful, e.g.,

$$\mathrm{Tp^*Ir}(\eta^2\text{-}\mathrm{C_2H_4})_2/60\ ^\circ\mathrm{C} \rightarrow \mathrm{Tp^*Ir}(\eta^2\text{-}\mathrm{C_2H_4})(\mathrm{H})(\eta^1\text{-}\mathrm{C_2H_3}) \rightarrow \mathrm{Tp^*Ir(H)}(\eta^3\text{-}\mathrm{CH_2CHCHMe})^{90}$$

(where Tp* = HB(3,5-dimethylpyrazoyl)$_3$)

The $^{13}C_2H_{3(ad)}$ then reacts with $\{^{12}CH_{2(ad)}\}$ from ^{12}CO to give the surface σ-allyl ($mCH_2{}^{13}CH{=}{}^{13}CH_2$, where m is the

(82) Vázquez de Miguel, A.; Isobe, K.; Bailey, P. M.; Meanwell, N. J.; Maitlis, P. M. *Organometallics* **1982**, *1*, 1604.
(83) [{CpRu(CO)}$_2$(μ_2-CO)(μ_2-CMe)]$^+$ + RCH=CH$_2$ → *cis*-[{CpRu(CO)}$_2$(μ_2-CO)(μ_2-CMe-CR=CH$_2$)] (R = H, Me): Dyke, A. F.; Guerchais, J. E.; Knox, S A R.; Roue, J.; Short, R. L.; Taylor, G E.; Woodward, P. *J. Chem. Soc., Chem. Commun.* **1981**, 537.
(84) For example, *cis*-[{Cp(CO)Fe}$_2$(μ-CO)(μ-CH)]$^+$ + CD$_2$=CD$_2$ → *cis*-[{Cp(CO)Fe}$_2$(μ-CO)(μ-CCD$_2$CD$_2$H)]$^+$ and *cis*-[{CpFe(CO)}$_2$(μ_2-CO)(μ_2-CH)]$^+$ + N$_2$CHR → *cis*-[{Cp(CO)Fe}$_2$(μ-CO)(μ-CH=CHR)]$^+$ (R = H, Me, CO$_2$Et, SiMe$_3$): Casey, C. P.; Fagan, P. J. *J. Am. Chem. Soc.* **1982**, *104*, 4950. Casey, C. P.; Meszaros, M W.; Fagan, P. J.; Bly, R. K.; Marder, S. R.; Austin, E. A. *J. Am. Chem. Soc.* **1986**, *108*, 4043. Casey, C. P.; Austin, E. A.; Rheingold, A. L. *Organometallics* **1987**, *6*, 2157.
(85) This links into olefin metathesis and also single site alkyl polymerization processes, see: Ittel, S. D.; Johnson, L. K.; Brookhart, M. *Chem. Rev.* **2000**, *100*, 1169. Evitt, E. R.; Bergman, R. G. *J. Am. Chem. Soc.* **1980**, *102*, 7003. Wang, L.; Flood, T. C. *J. Am. Chem. Soc.* **1992**, *114*, 3169.
(86) We are indebted to a referee for these suggestions, which were not in the original proposals; see ref 31.
(87) Maitlis, P. M. *J. Organomet. Chem.* **1995**, *500*, 239.
(88) Calhorda, M. J.; Brown, J. M.; Cooley, N. A. *Organometallics* **1991**, *10*, 1431.

Scheme 4

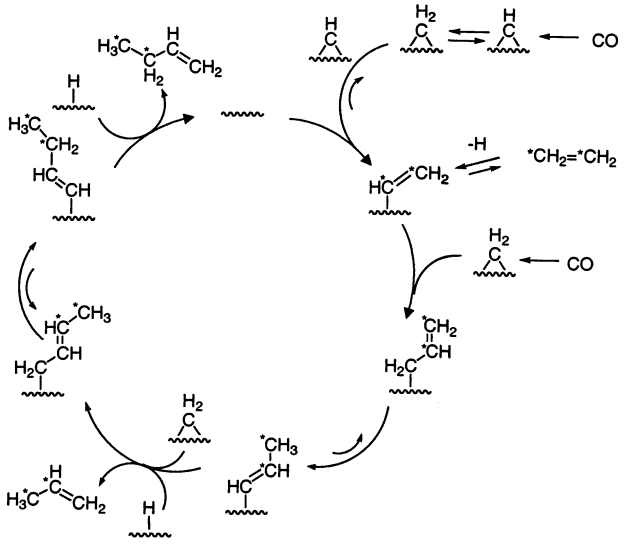

point of attachment to the metal surface), a sequence for which there are again good organometallic models.[91] To continue the reaction sequence in which an sp^2 C couples with a $\{CH_{2(ad)}\}$, an isomerization of the surface allyl to the 1-propenyl$_{(ad)}$ ($mCH{=}{}^{13}CH^{13}CH_3$) is then needed. Thereafter, the 1-propenyl$_{(ad)}$ can react in two ways: either to give $CH_2{=}{}^{13}CH^{13}CH_3$ on α-hydrogenolysis by $H_{(ad)}$ or to propagate by further reaction with $\{CH_{2(ad)}\}$. $CH_2{=}{}^{13}CH^{13}CH_3$ is the only propene isotopomer observed over Co and Ru at low temperatures, however, $^{13}CH_2{=}{}^{13}CHCH_3$ (vide infra) is also formed over Rh and Fe.

To involve the energetically favorable metal−C(sp^2) bonds in the next coupling, the σ-allyl$_{(ad)}$ formed in the previous step must first isomerize to a σ-1-propenyl. This step has been criticized, because it was claimed there was no good model for such a process.[92] In fact, that is not so; although concerted [1,3]-sigmatropic H-shifts are either forbidden[93] or sterically impracticable, many metal-assisted 1,3-H-shifts are known, and several organometallic reactions model allyl to 1-propenyl steps; for example:

$$CH_2{=}CMeCH_2Ir(L)_2(X)_2CO \rightarrow Me_2C{=}CHIr(L)_2(X)_2CO\ ^{94}$$

$$Cp^*{}_2Ta(\eta^3\text{-}C_3H_4) \rightarrow Cp^*{}_2Ta(CO)(\eta^1\text{-}CH{=}CHMe)\ ^{37}$$

$$Cp^*(TMF)Ti(\eta^3\text{-}C_3H_4) \rightarrow Cp^*(TMF)Ti(\eta^1\text{-}CH{=}CHMe)\ ^{95}$$

(where L = PMe_2Ph; Cp* = η^5-C_5Me_5;
TMF = η^4-tetramethylfulvene, $C_5Me_4{=}CH_2$)

Repetition of the steps of addition of $\{CH_{2(ad)}\}$ to a σ-1-alkenyl to give the homologous allyl, followed by another 1,3-H-shift to the homologous σ-1-alkenyl, allows the chain to grow by one CH_2 at a time. For example, $mCH{=}{}^{13}CH^{13}CH_3 \rightarrow mCH_2CH{=}{}^{13}CH^{13}CH_3$ (2-butenyl) $\rightarrow mCH{=}CH^{13}CH_2{}^{13}CH_3$ (1-butenyl), which, on reductive elimination, gives 1-butene with labeling, $CH_2{=}CH^{13}CH_2{}^{13}CH_3$; repetition of the steps gives higher members of the series, $CH_2{=}CH(CH_2)_n{}^{13}CH_2{}^{13}CH_3$, which are the species actually found.

It is suggested that chain termination and release of the 1-alkene product is by surface hydride attack on the alkenyl chain; a reaction equivalent to the organometallic reductive elimination, $RCH{=}CHmH \rightarrow RCH{=}CH_2$ (+m).[96]

The explanation offered by the alkenyl + $\{CH_{2(ad)}\}$ mechanism for the dip at C_2 in the Anderson−Schulz−Florey polymerization plots [of log(W/n) against n; where W is the mass fraction of polymers containing n monomer units] is that the precursor to C_2 products has a longer average lifetime than the precursors to higher hydrocarbons.[26,28−30] Thus, if the rate of initiation by the C_2 species is less than the rate of propagation, then this can decrease the amount of ethane and ethene produced.[97] Similarly, the amounts of methane formed need not lie on the ASF line, since its formation is not directly related to the polymerization steps needed to make the higher hydrocarbons.[98]

Suggestions to explain initiation in the absence of an added vinylic probe are summarized below.

Routes to 1-Alkenes $CH_2{=}{}^{13}CH^{13}CH_3$ and $CH_2{=}CH(CH_2)_n{}^{13}CH^{13}CH_3$ Based on Propagation by $\{CH_{(ad)} + H_{(ad)}\}$. Dynamic Monte Carlo and density functional theory calculations have led van Santen and his colleagues to propose views of the F−T polymerization process in which chain growth is by sequential addition of first surface CH and then H to a growing

(89) The alkenyl + $\{CH_{2(ad)}\}$ propagation step of the alkenyl mechanism should be energetically more favourable than the alkyl + $\{CH_{2(ad)}\}$ propagation step of the alkyl mechanism, as the latter can be viewed as an alkyl plus alkyl coupling, which is well-known to be very energetically demanding. See: Low, J. J.; Goddard, W. A. *J. Am. Chem. Soc.* **1984**, *106*, 6928 and 8321; *Organometallics* **1986**, *5*, 609; Trinquier, G.; Hoffmann, R. *Organometallics* **1984**, *3*, 370; Tatsumi, K.; Hoffmann, R.; Yamamoto, A.; Stille, J. K. *Bull. Chem. Soc. Jpn.* **1981**, *54*, 1857.

(90) Perez, P. J.; Poveda, M. L.; Carmona, E. *J. Chem. Soc. Chem., Commun.* **1992**, 8. Alvarado, Y.; Boutry, O.; Gutierrez, E.; Monge, A.; Nicasio, M. C.; Poveda, M. L.; Perez, P. J.; Ruiz, C.; Bianchini, C.; Carmona, E. *Chem. Eur. J.* **1997**, *3*, 860 and references therein. Bell, T. W.; Brough, S. A.; Partridge, M. G.; Perutz, R. N.; Rooney, A. D. *Organometallics*, **1993**, *12*, 2933. Stoutland, P. O.; Bergman, R. G. *J. Am. Chem. Soc.* **1985**, *107*, 4581. Stoutland, P. O.; Bergman, R. G. *J. Am. Chem. Soc.* **1988**, *110*, 5732.

(91) The vinyl plus methylene coupling is modeled by a variety of organometallic reactions, for example: Martinez, J. Gill, J. B.; Adams, H.; Bailey, N. A.; Saez, I. M.; Sunley, G. J.; Maitlis, P. M. *J. Organomet. Chem.* **1990**, *394*, 583. Jacobi, D.; Floriani, C.; Chiesi-Villa, A.; Rizzoli, C. *J. Am. Chem. Soc.* **1993**, *115*, 3595. Hill, A. F.; Ho, C. T.; Wilton-Ely, J. D. E. T. *Chem. Commun.* **1997**, 2207. Braun, T.; Gevert, O.; Werner, H. *J. Am. Chem. Soc.* **1995**, *117*, 7291. Werner, H.; Wiedemann, R.; Steinert, P.; Wolf, J. *Chem. Eur. J.* **1997**, *3*, 127. Fryzuk, M. D.; Gao, X. L.; Rettig, S. J. *J. Am. Chem. Soc.* **1995**, *117*, 3106. Fryzuk, M. D.; Gao, X. L.; Rettig, S. J. *Organometallics* **1995**, *14*, 4236. Wang, Z.-Q.; Maitlis, P. M. *J. Organomet. Chem.* **1998**, *569*, 85.

(92) The basis of the criticism seems to be because only decomposition (to uncharacterized solids and volatiles) rather than isomerization was observed when $[Fe(C_5R_5)(CO)_2(CH_2CH{=}CH_2)]$ (R = H, Me) was heated: Overett, M J.; Hill, R. O.; Moss, J. R. *Coord. Chem. Rev.* **2000**, *206−207*, 581. Ndlovu, S. B.; Phala, N. S.; Hearshaw-Timme, M.; Beagly, P.; Moss, J. R.; Claeys, M.; van Steen, E. *Catal. Today* **2002**, *71*, 343.

(93) Smith, M. B.; March, J. *March's Advanced Organic Chemistry*, 5th ed.; Wiley-Interscience: New York, 2001; p 1439.

(94) Deeming, A J.; Shaw, B. L.; Stainbank, R. E. *J. Chem. Soc. (A)* **1971**, 374.

(95) Brinkmann, P. H. P.; Luinstra, G. A.; Saenz, A. *J. Am. Chem. Soc.* **1998**, *120*, 2854.

(96) 1-Alkene formation in the alkyl + $\{CH_{2(ad)}\}$ mechanism is, in contrast, proposed to occur by β-elimination of H from an alkyl chain (Scheme 2). However, since β-elimination is in equilibrium with alkyl formation by the reverse reaction ($RCH{=}CH_2$ + mH ⇌ RCH_2CH_2m), it will be disfavored in the presence of hydrogen, a key component of the F−T reaction.

(97) An alternative possibility, that ethene, once formed is readsorbed and reenters the chain growth process (Komaya, T.; Bell, A. T. *J. Catal.* **1994**, *146*, 237. Dwyer, D J.; Somorjai, G A. *J Catal.* **1979**, *56*, 249), has been criticized because "similar participation would be likely in this case and no evidence of such participation is seen in the isotopic data".

(98) By contrast, if $^{13}C_2H_4$ were involved in the propagation steps rather than the initiation, then the linear hydrocarbons should show more than one pair of ^{13}C atoms and at different places; while if the $^{13}C_2H_4$ were involved in chain termination, then the pair of ^{13}C atoms should appear at the other (vinylic) end of the 1-alkenes.

Scheme 5

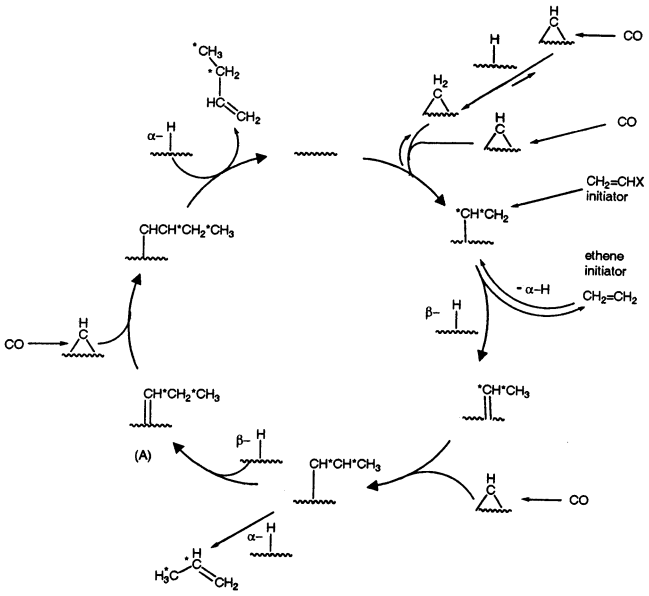

Scheme 6

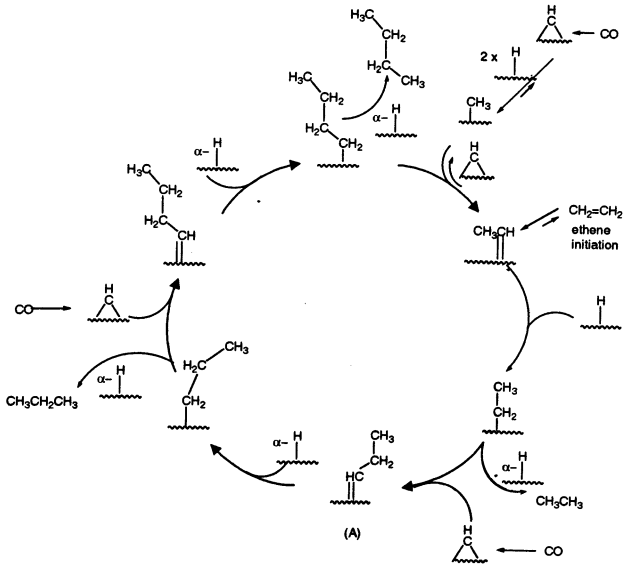

alkyl or to a growing alkylidene chain.[76 99] Representations of the alkylidene + $\{CH_{(ad)} + H_{(ad)}\}$ and alkyl + $\{CH_{(ad)} + H_{(ad)}\}$ cycles (adapted from those of van Santen and co-workers[76]) are given in Schemes 5 and 6, respectively.[100]

Scheme 5 shows the formation of propene ($^{13}CH_3{}^{13}CH{=}CH_2$) and of 1-butene ($^{13}CH_3{}^{13}CH_2CH{=}CH_2$) initiated by $^{13}C_2H_4$ and propagated by the alkylidene + $\{CH_{(ad)} + H_{(ad)}\}$ cycle. The first step is the formation of $\{CH_{2(ad)}\}$, which then reacts with $\{CH_{(ad)}\}$ to give a "vinyl-like" species, $\{CH_2CH_{(ad)}\}$, as previously proposed in the alkenyl + $\{CH_{2(ad)}\}$ mechanism. This then adds $H_{(ad)}$ β to give an ethylidene $\{CH_3CH_{(ad)}\}$, which in turn reacts again with $\{CH_{(ad)}\}$ to give $\{CH_3CHCH_{(ad)}\}$; alternatively, addition of $H_{(ad)}$ α to this or any other alkylidene$_{(ad)}$ releases the 1-alkene. Thus, the chain length is determined by the relative tendencies of $H_{(ad)}$ to add either α or β to the intermediate alkylidenes. Addition of $CH_2{=}CHX$ as probe generates $\{CH_2{-}CH_{(ad)}\}$ directly; the successive additions of $\{CH_{(ad)}\}$ then build up the hydrocarbon chain in a stepwise manner, and if the initiator is $^{13}C_2H_4$, then the $^{13}C_2$ labels will appear at the ethyl termini in the hydrocarbon products. "A" in Scheme 6 is where the alkylidene and the alkyl cycles intersect.

Routes to $CH_3{}^{13}CH{=}{}^{13}CH_2$ and Other 1-Alkene Isotopomers. In addition to the propene isotopomer $^{13}CH_3{}^{13}CH{=}CH_2$ formed over Co and Ru, an approximately equal amount of $CH_3{}^{13}CH{=}{}^{13}CH_2$ was formed over Fe and Rh. $CH_3{}^{13}CH{=}{}^{13}CH_2$ could be a secondary product that derives from the kinetically favored $^{13}CH_3{}^{13}CH{=}CH_2$ by a 1,3-hydrogen shift. However, such an isomerization of a *first formed* alkene by a 1,3-hydrogen shift must be relatively slow, with respect to the time that the reaction products are in contact with the catalyst, since our other data show that the thermodynamically favored internal olefins are almost always minor products from the F−T reactions.[55] Even over Co at 220 °C, a highly hydrogenating system where the major products are methane and alkanes, the ratio of 2-butenes to 1-butene is found to be only around 1, compared to an expected value of ca. 6.5 at equilibrium (Table 3).

While the spectra in the =CH− region (δ ~133.7) of the propene produced over Ru/150 °C or Co/180 °C show that the isotopomer formed was $^{13}CH_3{}^{13}CH{=}CH_2$, as the reaction temperature was increased (to 180 °C for Ru, and 220 °C for Co; Figures 1 and 2) only a very small amount of $CH_3{}^{13}CH{=}{}^{13}CH_2$ grew in,[101] and the major new species seen were the mono-^{13}C labeled $CH_3{}^{13}CH{=}CH_2$ and the trilabeled $^{13}CH_3{}^{13}CH{=}{}^{13}CH_2$. This result indicates that, *once formed*, the propene isotopomer $^{13}CH_3{}^{13}CH{=}CH_2$ does not *readily* rearrange to $^{13}CH_2{=}{}^{13}CHCH_3$.

Since the products are largely kinetically controlled, paths are needed that lead directly to $CH_3{}^{13}CH{=}{}^{13}CH_2$ over Rh and Fe. A characteristic differentiating the Ru- or Co-catalyzed from the Rh- or Fe-catalyzed reactions is that the chain growth probability (α) is significantly smaller for Rh and Fe ($\alpha \sim 0.4$) than for Ru and Co ($\alpha \sim 0.6$; Table 1). This indicates that one or more steps in the chain growth are more difficult (slower) for Fe and Rh and that other steps, for example, hydrogenolysis of a surface allyl, now compete.

The alkenyl + $\{CH_{2(ad)}\}$ scheme can accommodate this. If the intermediate allylic surface species, $CH_2{=}CHCH_2$m (when m = Co or Ru), is transformed rapidly into the 1-propenyl $CH_3{-}CH{=}CH$m, the polymerization continues. However, if the allylic species $CH_2{=}CHCH_2$m is slow to rearrange and react with more methylene, hydrogenolysis can occur instead. If initiation is by $^{13}CH_2{=}{}^{13}CH$m, this gives rise to $^{13}CH_2{=}{}^{13}CHCH_3$ (when m = Fe or Rh),

$$^{13}CH_2{=}{}^{13}CH\text{m} + \{CH_{2(ad)}\} \rightarrow {}^{13}CH_2{=}{}^{13}CHCH_2\text{m} \rightarrow {}^{13}CH_2{=}{}^{13}CHCH_3$$

(99) The addition of $\{CH_{(ad)} + H_{(ad)}\}$ to an alkyl chain is a variant of the Brady−Pettit alkyl + methylene mechanism, while the addition of $\{CH_{(ad)} + H_{(ad)}\}$ to an alkylidene chain is effectively a variant of the alkenyl + $\{CH_{2(ad)}\}$ mechanism that our group has proposed and of the alkylidene−hydride−alkenyl mechanism of Gibson et al.

(100) Ciobica and van Santen have included other surface species such as triply coordinated alkylidynes ($RC{\equiv}_{(ad)}$) and have also linked the F−T mechanism to methane homologation in their schemes. For simplicity and since these paths are of less relevance to the studies described here, we have not included them.

(101) The ^{13}C NMR spectrum of propene formed over Ru at 180 °C shows that the ratio of $^{13}CH_2{}^{13}CH{=}CH_2$ to $CH_2{}^{13}CH{=}{}^{13}CH_2$ is around 5:1, and over Co at 220 °C the ratio is around 1.2:1, but it must be noted that there are much larger amounts of $CH_2{}^{13}CH{=}CH_2$ and $^{13}CH_2{}^{13}CH{=}{}^{13}CH_2$ present.

As fast 1,3-H shifts involving coordinated species (e.g. of surface allyl to propenyl) are integral to the alkenyl + $\{CH_{2(ad)}\}$ mechanism, it is the recoordination of the olefin, once it has been formed, that must be unfavorable.[102]

By contrast, as 1,3-H shifts are not integral to the alkylidene + $\{CH_{(ad)} + H_{(ad)}\}$ mechanism, an extra isomerization, $mCH{=}{}^{13}CH^{13}CH_3 \rightarrow CH_3{}^{13}CH{=}{}^{13}CHm$, must occur over Rh and Fe, but not over Ru and Co, for the formation of $CH_3{}^{13}CH{=}{}^{13}CH_2$ by a primary process. As this does not correlate with a step in the cycle that can become slow, the reason such an isomerization should occur is not clear. For similar reasons, the formation of $CH_3{}^{13}CH{=}{}^{13}CH_2$ by a primary process based on the alkyl + $\{CH_2\}_{(ad)}$ mechanism is not readily explained.

The NMR data relating to the higher temperature reactions show that 1-alkenes containing one ^{13}C and three ^{13}C's are also formed. While a part of the $^{13}C_1$ that is found comes from natural abundance in ^{12}CO, most arises from the $^{13}C_2H_4$ probe molecule by cleavage, to give $\{^{13}CH_{2(ad)}\}$. For example, the high-temperature reaction products over Ru or Co contain the three propene-$^{13}C_1$ isotopomers and the propene-$^{13}C_3$. Similarly, the 1-butene contains (i) all the four 1-butene-$^{13}C_1$ isotopomers, (ii) $^{13}CH_3{}^{13}CH_2{}^{13}CH{=}{}^{13}CH_2$, (iii) $^{13}CH_3{}^{13}CH_2{}^{13}CH{=}CH_2$ and $^{13}CH_3{}^{13}CH_2CH{=}{}^{13}CH_2$, and (iv) $CH_3CH_2{}^{13}CH{=}{}^{13}CH_2$, in addition to the chief lower reaction temperature isotopomer, $^{13}CH_3{}^{13}CH_2CH{=}CH_2$.

The alkenyl + $\{CH_2\}_{(ad)}$ scheme can readily explain the formation of the various alkene-$^{13}C_1$ (and $^{13}C_3$) products. Both isotopomeric $\{CH_{2(ad)}\}$ will be incorporated randomly into the growing polymers when a $\{^{13}CH_{2(ad)}\}$ derived from either $^{13}CH_3$-NO_2 or by cleavage of a $^{13}CH_2{=}{}^{13}CH_2$ probe mixes with $\{^{12}CH_{2(ad)}\}$ derived from CO. Thus, if a $^{12}CH_{2(ad)}$ adds to a $^{13}C_2H_{3(ad)}$ species, the end result will be $^{13}CH_3{}^{13}CH{=}CH_{2(ad)}$; if a $^{13}CH_{2(ad)}$ adds to a $^{13}C_2H_{3(ad)}$ species, the final product will be $^{13}CH_3{}^{13}CH{=}{}^{13}CH_2$; if a $^{12}CH_{2(ad)}$ adds to a $^{12}C_2H_{3(ad)}$ species, the final product will be *all*-^{12}C $CH_3CH{=}CH_2$, while if a $^{13}CH_{2(ad)}$ adds to a $^{12}C_2H_{3(ad)}$ species, the product will be CH_3-$CH{=}{}^{13}CH_2$. There will also be a route to a mixed $^{13}C^{12}C$ initiator from the $^{13}C_1$ and the $^{12}C_1$ related to the mechanism for generating $^{12}C_2$ species in the absence of a special probe, which can account for the other propene-$^{13}C_1$ isotopomers found.

Paths to $^{13}C_1$- and $^{13}C_3$-containing products can also be proposed based on the alkyl + $\{CH_2\}_{(ad)}$ and on the alkylidene + $\{CH_{(ad)} + H_{(ad)}\}$ schemes if $CH_2{=}CH_2$, $CH_2{=}CHX$, and CH_3NO_2 probes can all generate $\{CH_{(ad)}\}$.

Routes to 2-Alkenes. The 2-butenes formed with added $^{13}C_2H_4$ probe under mild conditions contain either four ^{13}C or two ^{13}C atoms, $^{13}CH_3{}^{13}CH{=}CHCH_3$. As suggested previously,[22,103] the 2-butene-$^{13}C_4$ must arise from probe dimerization, possibly according to

$$^{13}CH_2{=}{}^{13}CH_{(ad)} + {}^{13}CH{=}{}^{13}CH_{2(ad)} \rightarrow {}^{13}CH_2{}^{13}CH^{13}CH^{13}CH_{2(ad)}$$

$$^{13}CH_2{}^{13}CH^{13}CH^{13}CH_{2(ad)} + 2\,H_{(ad)} \rightarrow {}^{13}CH_3{}^{13}CH{=}{}^{13}CH^{13}CH_3$$

The dilabeled 2-butene is mainly $^{13}CH_3{}^{13}CH{=}CHCH_3$. If it arises as a secondary product, that would be from $^{13}CH_3{}^{13}CH_2$-$CH{=}CH_2$ by a 1,3-H-shift. If a part arises as a primary product, the alkenyl + $\{CH_{2(ad)}\}$ mechanism offers a path very similar to the surface allyl hydrogenolysis forming $^{13}CH_2{=}{}^{13}CH{-}CH_3$, but one step further on, namely,

$$^{13}CH_3{}^{13}CH{=}CH_{(ad)} + \{CH_{2(ad)}\} \rightarrow {}^{13}CH_3{}^{13}CH{=}CH{-}CH_{2(ad)}$$

Then, instead of isomerizing to the 1-butenyl, which hydrogenolyzes to the 1-butene, the 2-butenyl intermediate can be directly hydrogenolyzed to give the internal butene,

$$^{13}CH_3{}^{13}CH{=}CH{-}CH_{2(ad)} + H_{(ad)} \rightarrow {}^{13}CH_3{}^{13}CH{=}CHCH_3$$

Thus, the dilabeled 1- and 2-butenes are predicted to be $^{13}CH_3{}^{13}CH_2CH{=}CH_2$ and $^{13}CH_3{}^{13}CH{=}CHCH_3$, respectively; these isotopomers were found over all the metals investigated. The above arguments can be extended to explain the formation of the di- and tetralabeled higher 2-alkenes, $^{13}CH_3{}^{13}CH{=}CHCH_2R$ and $^{13}CH_3{}^{13}CH{=}{}^{13}CH^{13}CH_2R$, when initiated with labeled vinyl, $^{13}CH_2{=}{}^{13}CH_{(ad)}$.

Since the formation of the 2-alkenes as primary products involves allylic intermediates, as for $^{13}CH_2{=}{}^{13}CHCH_3$, this is again less readily rationalized on the basis of either the alkyl + $\{CH_{2(ad)}\}$ or the alkylidene + $\{CH_{(ad)} + H_{(ad)}\}$ schemes.

Routes to Methylalkenes. Although branched chain olefins were very minor products in our experiments, some (especially 2-methyl-2-butene and 2-methyl-2-pentene) are formed and they have been reported to become major products when the reactions were carried out under more vigorous conditions.[25] This suggests that some arise by skeletal rearrangements promoted by the catalyst and support in secondary reactions. However, 1,2-shifts of the metal/point of attachment of intermediates of either the alkyl + $\{CH_{2(ad)}\}$ or the alkenyl + $\{CH_{2(ad)}\}$ mechanism[104] can offer a direct entry to methylalkenes (Supporting Information).

Routes to Alkanes. Similarly to the 1-alkenes, the *n*-alkanes formed using $^{13}C_2H_4$ probes contain considerable double labeling in the ethyl tails and very little elsewhere. A comparison of the pfr's of alkanes and 2-alkenes with those of 1-alkenes for different chain lengths and at different flow rates (Supporting Information) indicates that a large proportion of the alkanes and the 2-alkenes are secondary products formed from the 1-alkenes in subsequent steps.[105] The alkenyl + $\{CH_{2(ad)}\}$ mechanism offers no simple direct routes to *n*-alkanes, which accords well with our experimental observations. It is found that alkanes become more important for longer chain products. This can be understood if longer 1-alkenes hydrogenate more readily under F−T conditions; it has been suggested that longer chain alkenes are held up in the reactor, leading to longer residence times and resulting in more hydrogenation.[10,55,106]

By contrast, however, the alkyl + $\{CH_{2(ad)}\}$ cycle (Scheme 2) can lead directly to n-alkanes if the surface alkyl intermediates are hydrogenolyzed. The alkyl + $\{CH_{(ad)} + H_{(ad)}\}$ cycle also leads directly to alkanes if the termination step is again by

(102) Such situations are well-known; see, for example: Bond, G. C.; Wells, P. B. *Adv. Catal.* **1964**, *15*, 91.

(103) For a related reaction, see: Leconte, M.; Theolier, A.; Basset, A. *J. Mol. Catal.* **1985**, *28*, 217.

(104) Wang, L.-S.; Cowie, M. *Can. J. Chem.* **1995**, *73*, 1058.

(105) Several authors have shown that alkenes are readily hydrogenated to alkanes under F−T conditions: Kuipers, E. W.; Scheper, C.; Wilson, J. H.; Vinkenburg, I. H.; Oosterbeek, H. *J. Catal.* **1996**, *158*, 288.

(106) Kuipers, E. W.; Vinkenburg, I. H.; Oosterbeek, H. *J. Catal.* **1995**, *152*, 137.

reductive elimination with surface hydride as in Scheme 6,[107] adapted from that of van Santen and co-workers.[76]

The alkenyl + $\{CH_{(ad)} + H_{(ad)}\}$ and the alkyl + $\{CH_{(ad)} + H_{(ad)}\}$ cycles share common alkylidene intermediates (labeled A in Schemes 5 and 6), and the existence of two associated cycles, one leading to *n*-alkenes and the other to *n*-alkanes, would allow the actual products to be controlled by the conditions used for the reactions.

Formation of $CH_{2(ad)}$ or $CH_{(ad)}$. Current thinking suggests that formation of the putative $CH_{2(ad)}$ or $CH_{(ad)}$ from CO involves the deoxygenation of CO to give a surface carbide, followed by a stepwise hydrogenation. The deoxygenation step is found in the formation of carbides from carbonyl clusters[108,109] and in other model organometallic reactions.[110,111] Although stoichiometric reactions of coordinated CO with H_2 to give directly CH_2 or CH liganded to a metal have not yet been reported, such reductions using $LiAlH_4$, $NaBH_4$,[112] or hydrosilanes[113] and the addition of H to a metal carbide giving either a methylidyne $CH_{(ad)}$ or a methylene $CH_{2(ad)}$ are known.[80,114,115]

Since model organometallic complexes indicate facile equilibration between CH_2 and CH ligands, it is likely that this will also be true for surface species. Thus, whether chain propagation occurs as a single step (Scheme 4) or in two steps (Scheme 5) will be determined by the relative energetics of combination of the $C_{1(ad)}$ species and the growing chain and by the equilibrium

$$CH_{2(ad)} \rightleftharpoons CH_{(ad)} + H_{(ad)}$$

Further research to define more completely both the C_1 and the C_2 species on metal surfaces in the presence of hydrogen and their reactivity in model organometallic systems is urgently needed.

Several workers have commented that in the catalytic heterogeneous F−T reaction the formation of the $C_{1(ad)}$ species from adsorbed CO and surface hydrogen (Scheme 1) proceeds very rapidly and is not rate-determining;[26,30] the slow step is then associated with the initiation of polymerization; our data are entirely in agreement with this view.

Initiation in the Absence of a Vinylic Probe. The results of Bell and Mims and their co-workers show that the C_2 initiator can also be formed directly from CO in catalytic reactions. Spectroscopic studies of the species generated from hydrocarbons on clean metal surfaces in vacuo suggest some analogies in that $\{CH_{(ad)}\}$ reacts with surface carbon $\{C_{(ad)}\}$, giving $\{CCH_{(ad)}\}$ by about 450 K,[72−74] a temperature within the range of a F−T reaction; $\{CCH_{(ad)}\}$ would appear to be a surface acetylide $\{HC{\equiv}C_{(ad)}\}$, which could presumably be hydrogenated to a vinylidene or a vinyl. Surface vinylidene $\{CH_2{=}C{=}_{(ad)}\}$ and ethylidyne $\{CH_3C{\equiv}_{(ad)}\}$ have also been detected at 500−550 K and below 400 K, respectively, over Ru.[74] In a catalytic system, in the absence of an added vinylic probe, the initiator could arise by combination of a methylidyne and a methylene, $CH_{(ad)} + CH_{2(ad)} \rightarrow CH{=}CH_{2(ad)}$;[21] a related organometallic reaction has been reported for a trinuclear cluster complex.[116] An alternative possibility is that the C_2 initiator arises from a metal carbonyl via surface-supported carbide or dicarbide carbonyl clusters. Shapley[109] and Chini[108] and their co-workers have shown that such carbide clusters form very easily, in some cases under thermal conditions[117]

$$Ru_6(CO)_{18}{}^{2-}/\text{diglyme}/162\ ^\circ\text{C} \rightarrow Ru_6C(CO)_{16}{}^{2-}$$

$$Ru_6C(CO)_{16}{}^{2-}/\text{tetraglyme}/220\ ^\circ\text{C} \rightarrow [Ru_{10}(C)_2(CO)_{24}]^{2-}$$

Conclusions

^{13}C NMR spectroscopy has shown that CO hydrogenation, over four catalysts under mild conditions of temperature (Ru/150 °C, Co/180 °C, Rh/190 °C, and Fe/ 220 °C) and pressure (1 atm; CO:H_2, 1:1), in the presence of $^{13}C_2H_4$ probes leads to 1-alkenes as primary products, with $^{13}CH_3{}^{13}CH_2-$ labeling at the alkyl ends. To explain the similarity of product distribution, very similar reactions must occur over all the four metals, though at somewhat differing rates. *n*-Alkanes and internal olefins, as well as traces of branched chain olefins and oxygenates,[48] are produced in addition to the 1-alkenes. The *n*-alkanes and the internal *n*-alkenes produced in these experiments also show $^{13}CH_3{}^{13}CH_2-$ labeling in the alkyl tails; they appear to arise mainly by secondary hydrogen addition or migration reactions from the 1-alkenes.

The products are formed by the polymerization of $C_{1(ad)}$ species derived from CO. Four different schemes have been suggested to explain the formation of 1-alkenes in terms of surface methylenes$\{CH_{2(ad)}\}$ adding to the chain in a single step: the alkyl + $\{CH_{2(ad)}\}$,[31] the alkenyl + $\{CH_{2(ad)}\}$, the alkylidene−hydride−alkenyl + $\{CH_{2(ad)}\}$,[37] and the metathesis-type metallacyclobutane/$\{CH_{2(ad)}\}$ mechanisms.[38,85] The results presented here argue against the alkylidene−hydride−alkenyl + $\{CH_{2(ad)}\}$, and the metathesis-type metallacyclobutane/$\{CH_{2(ad)}\}$ schemes as they have been formulated.

Although the popular alkyl + $\{CH_{2(ad)}\}$ mechanism as originally formulated can explain the formation of 1-*n*-alkenes

(107) This shows the formation of terminally labeled alkanes, ($^{13}CH_3{}^{13}CH_2-$R) initiated by $^{13}C_2H_4$ and propagated by $\{CH_{(ad)} + H_{(ad)}\}$. The first step is again the formation of a surface C_2 species by combination of two C_1 species (in this case $CH_3CH_{(ad)}$ from $CH_{3(ad)} + CH_{(ad)}$): this step must also be reversible to allow for the label scrambling seen at high temperatures. Subsequent steps involve addition of $\{CH_{(ad)}\}$ to surface alkyls $\{RCH_{2(ad)}\}$, giving alkylidenes $RCH_2CH_{(ad)}$ which then react with $H_{(ad)}$ to give the homologous alkyl, $RCH_2CH_{2(ad)}$, and so forth. Chain termination to give the alkane RCH_2CH_3 is proposed to occur by α-addition of $H_{(ad)}$.

(108) Albano, V. G.; Chini, P.; Martinengo, S.; Sansoni, M.; Strumolo, D. *J. Chem. Soc., Dalton Trans.* **1978**, 459.

(109) Tai Hayward, C.-M.; Shapley, J R.; Churchill, M.; Bueno, C.; Rheingold, A. L. *J. Am. Chem. Soc.* **1982**, *104*, 7347.

(110) Miller, R. L.; Wolczanski, P T.; Rheingold, A. L.. *J. Am. Chem. Soc.* **1993**, *115*, 10422. Neithamer, D. R.; LaPointe, R. E.; Wheeler, R. A.; Richeson, D S.; Van Duyne, G. D.; Wolczanski, P. T. *J. Am. Chem. Soc.* **1989**, *111*, 9056. Chisholm, M. H.; Hammond, C. E.; Johnston, V. J.; Streib, W. E.; Huffman, J. C. *J. Am. Chem. Soc.* **1992**, *114*, 7056. Calderazzo, F.; Englert, U.; Guarini, A.; Marchetti, F.; Pamploni, G.; Segre, A. *Angew. Chem., Int. Ed. Engl.* **1994**, *33*, 1188. Caselli, A.; Solari, E.; Scopelliti, R.; Floriani, C. *J. Am. Chem. Soc.* **2000**, *122*, 538.

(111) H-exchange between methylidyne and methylene within a complex is well-documented: Lee, K.; Wilson, S. R.; Shapley, J. R. *Organometallics* **1998**, *17*, 4113. Hamilton, D. H.; Shapley, J. R. *Organometallics* **2000**, *19*, 761. Zaera, F. *Chem. Rev.* **1995**, *95*, 2651.

(112) Brown, S L.; Davies, S. G. *J. Organomet. Chem.* **1984**, *268*, C53. Davies, S. G.; Simpson, S. J. *J. Chem. Soc., Chem. Commun.* **1986**, 84.

(113) Akita, M.; Oku, T.; Moro-oka, Y. *J. Chem. Soc., Chem. Commun.* **1992**, 1031.

(114) Etienne, M.; White, P. S.; Templeton, J. L. *J. Am. Chem. Soc.* **1991**, *113*, 2324. Jamison, G. M.; Bruce, A. E.; White, P. S.; Templeton, J. L. *J. Am. Chem. Soc.* **1991**, *113*, 5057. Greco, J. B.; Peters, J. C.; Baker, T. A.; Davis, W. M.; Cummins, C. C.; Wu, G. *J. Am. Chem. Soc.* **2001**, *123*, 5003. See also: Herrmann, W. A.; Plank, J.; Guggolz, E.; Ziegler, M. L. *Angew. Chem.* **1980**, *92*, 660.

(115) Another functionalization of a cluster carbide has been reported: Bradley, J. S. *Adv. Organomet. Chem.* **1983**, *22*, 1.

(116) Davies, D. L.; Parrott, M. J.; Sherwood, P.; Stone, F. G. A. *J. Chem. Soc., Dalton Trans.* **1987**, 1201.

(117) Templeton et al. have also reported the spontaneous dimerization of Tp*M-$(CO)_2{\equiv}$CH to $Tp^*(CO)_2M(\mu\text{-}CCH_2)M(CO)_2Tp^*$: Jamison, G. M.; Bruce, A. E.; White, P. S.; Templeton, J. L. *J. Am. Chem. Soc.* **1991**, *113*, 5057.

and *n*-alkanes, and some features of the labeling found when the reaction is initiated by a $^{13}C_2H_4$ probe, many of the experimental data can only be reconciled with it if substantial modifications are added to the original mechanism. The best of these then resemble the alkylidene/alkyl + $\{CH_{(ad)} + H_{(ad)}\}$ paths (vide infra).

The information presently at hand indicates that the alkenyl + $\{CH_{2(ad)}\}$ reaction[21] (Scheme 3) accounts most satisfactorily for the details of hydrocarbon formation. In this mechanism, it is proposed that the polymerization is initiated by a $C_{2(ad)}$ initiator, formulated as a surface vinyl, $CH_2{=}CH_{(ad)}$. The initiator can be formed even in the absence of a C_2 probe, and comparisons indicate that addition of the ethene probe has no major effect on the reaction path.

The alkenyl + $\{CH_{2(ad)}\}$ mechanism agrees well with the labeling studies and ties in with the traditional view of the F−T reaction. It explains the formation of the unusual isotopomer $^{13}CH_2{=}^{13}CHCH_3$ and internal alkenes, as well as methylalkenes, as primary products; the reason why vinylic (but not ethyl) probes can initiate; and the shape of the Anderson−Schulz−Florey polymerization plots. It is also consistent with other data indicating that C−C coupling involving σ-alkenyl−metal intermediates is more facile than for alkyl−metal species.

The regiospecific formation of 1-alkenes with $^{13}CH_3{}^{13}CH_2-$ tails is also explained by the alkylidene + $\{CH_{(ad)} + H_{(ad)}\}$ path recently proposed by van Santen and his colleagues, (Scheme 5).[76] A related alkyl + $\{CH_{(ad)} + H_{(ad)}\}$ mechanism (Scheme 6) can account for any primary *n*-alkane formation, as can the alkyl + $\{CH_{2(ad)}\}$ scheme. However, since alkanes are largely formed in secondary processes by hydrogenation of the alkenes, a direct route may be of less importance.

The methylidyne intermediates proposed in the two-step schemes appear to correlate with $\{CH_{(ad)}\}$ species found on clean metal surfaces in vacuo, but while studies indicate that $\{CH_{2(ad)}\}$ is less stable than $\{CH_{(ad)}\}$ on clean surfaces in vacuo, there are as yet no data on the effect that an atmosphere of hydrogen, associated with much surface hydride, has on the nature of the C_1 surface species. Organometallic model complexes show there is considerable mobility of hydrogen between methylidyne and methylene and between vinyl and vinylidene ligands. Thus, whether the homologation occurs as a single step (Scheme 3) or in two steps (Scheme 5) will be determined by the relative energetics of combination of the $C_{1(ad)}$ species and the growing chain and by the equilibrium

$$CH_{2(ad)} \rightleftharpoons CH_{(ad)} + H_{(ad)}$$

Since, by definition, critical intermediates in catalytic reactions are expected to be highly reactive, the fact that the surface studies suggest that $\{CH_{2(ad)}\}$ is *less* stable than $\{CH_{(ad)}\}$ could indicate that $\{CH_{2(ad)}\}$ is a *more* reactive intermediate than $\{CH_{(ad)}\}$ and hence more likely to participate in reactions. One possibility, therefore, is that on the surface there is a dynamic equilibrium between methylidyne hydride and methylene species, where the methylene is the reactive form, while the μ_3-methylidyne is the "resting state".

This study also indicates that relatively simple metal catalysts, even when unmodified and unpromoted, can give highly regiospecific reactions. Complications only arise at higher temperatures when secondary processes leading to isomerization and cleavage reactions begin to be significant.

Acknowledgment. We thank Sue Bradshaw and Brian Taylor for NMR spectra; Simon Thorpe for help with GC instrumentation; the EPSRC, the Royal Society, the ORS, and Center Grand, Department of Chemistry, Institut Teknologi Bandung, Indonesia, for financial support; Valerio Zanotti for advice; and Rutger van Santen for a copy of the PhD thesis of I. M. Ciobica.

Supporting Information Available: Eleven figures (^{13}C NMR spectra; pfr's), three reaction schemes, and eight tables (pfr's and reference NMR data). This material is available free of charge via the Internet at http://pubs.acs.org.

JA026280V